

5-2018

Preclinical Evaluation of Matrix Metalloproteinase Inhibitors and Protein Kinase C Activators in Cell and Mouse Models of Huntington's Disease

Kuruwitage Madushani
Dominican University of California

<https://doi.org/10.33015/dominican.edu/2018.bio.02>

Survey: Let us know how this paper benefits you.

Recommended Citation

Madushani, Kuruwitage, "Preclinical Evaluation of Matrix Metalloproteinase Inhibitors and Protein Kinase C Activators in Cell and Mouse Models of Huntington's Disease" (2018). *Graduate Master's Theses, Capstones, and Culminating Projects*. 333. <https://doi.org/10.33015/dominican.edu/2018.bio.02>

This Master's Thesis is brought to you for free and open access by the Student Scholarship at Dominican Scholar. It has been accepted for inclusion in Graduate Master's Theses, Capstones, and Culminating Projects by an authorized administrator of Dominican Scholar. For more information, please contact michael.pujals@dominican.edu.

**Preclinical Evaluation of Matrix Metalloproteinase Inhibitors and
Protein Kinase C Activators in Cell and Mouse Models of Huntington's Disease**

By

Kuruwitage Lakshika Madushani

A culminating thesis submitted to the faculty of Dominican University of California in
partial fulfillment of the requirements for the degree of Master of Science in Biology

San Rafael, California

May, 2018

This thesis, written under the direction of candidate's thesis advisor and approved by the thesis committee and the MS Biology program director, has been presented and accepted by the Department of Natural Sciences and Mathematics in partial fulfillment of the requirements for the degree of Master of Science in Biology at Dominican University of California. The written content presented in this work represent the work of the candidate alone.

Kuruwitage Lakshika Madushani

Candidate 05/11/2018

Lisa M. Ellerby, Ph.D.

Thesis Advisor 05/11/2018

Robert Barr, Ph.D.

Second Reader 05/11/2018

Meredith Protas, Ph.D.

Program Director 05/11/2018

Copyright © 2018, by Kuruwitage Lakshika Madushani

All rights reserved

Table of Contents

ABSTRACT:	VI
SPECIFIC AIMS:	VII
ACKNOWLEDGEMENTS:	IX
CHAPTER 1	1
ABSTRACT:	1
INTRODUCTION:	2
METHODS:	7
<i>Cell Culture</i>	7
<i>Western Blot Analysis</i>	7
<i>Immunocytochemistry</i>	8
<i>Caspase-3/7 Assay</i>	9
<i>Pharmacokinetic Mouse Study</i>	9
<i>Gelatin Zymography</i>	10
<i>Enzymatic Assay</i>	11
RESULTS:	11
DISCUSSION:	16
TABLES AND FIGURES:	24
<i>Table 1: Structure and Classification of MMPs and TIMPs</i>	24
<i>Table 2: Structure and PK Parameters of MMP Inhibitor Compounds</i>	25
<i>Figure 1: Increased Expression of MMP-3/10 in HD-NSCs</i>	26
<i>Figure 2: Decreased Expression of MMP-14 in HD-NSCs</i>	27
<i>Figure 3: Altered MMP-2 and MMP-9 Activity and Localization in HD-NSCs</i>	28
<i>Figure 4: TIMP-1 Expression in HD-NSCs</i>	30
<i>Figure 5: 9j, 19v, 19w are Neuroprotective in Mouse Striatal Cells</i>	31
<i>Figure 6: Pharmacokinetic Profile of MMP Inhibitor Compounds: 9j, 19v, and 19w</i>	32
<i>Figure 7: Visualization of MMP-2 and MMP-9 Activity by Gelatin Zymography</i>	33
<i>Figure 8: Measurement of MMP-2 Activity by Enzymatic Assay of Fluorogenic Substrate</i>	34
<i>Figure 9: Gelatin Zymogram of MMP Inhibitor Administered Mice</i>	35
<i>Figure 10: MMP-2 Expression of MMP Inhibitor Administered Mice</i>	36
<i>Figure 11: MMP-9 Expression in MMP Inhibitor Administered Mice</i>	37
CHAPTER 2	38
ABSTRACT:	38
INTRODUCTION:	39
METHODS:	41
<i>Drug Dosage Treatment</i>	41
<i>Caspase-3/7 Assay</i>	42
<i>Western Blot</i>	42
<i>Rotarod</i>	43
<i>Open Field</i>	43

<i>Hind Limb Claspings</i>	43
RESULTS:	44
DISCUSSION:	46
TABLES AND FIGURES:.....	49
<i>Figure 12: Cytotoxicity Evaluated in Striatal Hdh^{111Q/111Q} cells and HD-NSCs</i>	49
<i>Figure 13: Bryostatin-1 Dosage Response via IP and IV Route</i>	50
<i>Figure 14: Behavioral Study of Bryostatin-1 Treated R6/2 Mice</i>	51
<i>Figure 15: Open Field Testing of Bryostatin-1 Treated R6/2 mice</i>	52
REFERENCES	54

Abstract:

Huntington's disease (HD) is an incurable genetic neurological disorder that affects 1 in 10,000 people, with no treatment that can alter the course of the disease. Neural cell death in the striatum and the cortex results from the accumulation of toxic mutant huntingtin protein (mHTT) fragments. Full length HTT is cleaved by proteases, including caspases, calpains and matrix metalloproteinases (MMPs). Previous research has also shown altered kinase signaling pathways in HD contribute to the localization of mutant huntingtin to the nucleus and to disruption of transcriptional regulation. Currently, there are no drugs that delay the onset or slow the progression of Huntington's disease. We hypothesized that known drugs that target specific enzymes that have been evaluated in cancers and other neurological diseases may have therapeutic benefit in HD. Such enzymes that have been evaluated are MMP inhibitors and PKC activators, both enzymes that have been known to impact proteolytic processing and localization of mutant huntingtin. We evaluated these previously established compounds and their effect in HD mouse striatal cells, human neural stem cells, and transgenic mouse models. We have evaluated three MMP inhibitor compounds and found one that crosses the blood brain barrier and as predicted inhibits gelatinases. We have also found the PKC activator, Bryostain-1, increased the average life span in HD R6/2 treated mice.

Specific Aims:

Aim 1: *Prior evaluation of MMP in HD cellular models and transgenic mouse models have shown dysregulated MMP expression and activity in diseased compared to control samples. MMP dysregulation has also been demonstrated in post-mortem HD patient tissue as well as cerebrospinal fluid samples of HD patients. The first aim is to investigate the expression of MMP members, MMP-3/10, MMP-14, MMP-2, MMP-9, and their localization in patient-derived HD neural stem cells (HD-NSC) and compare against the CAG-corrected NSC line (C116-NSC). The dysregulation of MMP expression in human HD neural stem will be studied using immunoblotting techniques and RT-PCR.*

Aim 2: *Pharmacological inhibitors of MMP (9j, 19v, and 19w) will be utilized to study the substrate-specific inhibition of MMP class members, gelatinases, to evaluate the biochemical changes in the brain of C57/BL6 mice. Penetration of 9j, 19w, and 19v across the blood-brain barrier (BBB) from blood to brain tissue will be evaluated by LC/MS in conjunction with a pharmacokinetic study. Biochemical changes will be evaluated via gelatin zymography and MMP enzymatic assays using fluorogenic substrate.*

Aim 3: *PKC activation has been shown to offer potential therapeutic benefit in neurodegenerative diseases, including Alzheimer's Disease and Multiple Sclerosis. Bryostain-1, a PKC activator, will be evaluated to determine any beneficial improvements in locomotor deficits and other behavioral phenotypes in HD R6/2 transgenic mouse model. This will be evaluated using rotarod, open field behavioral*

assays and hind limb clasping assay to monitor locomotor phenotype associated with disease progression.

Acknowledgements:

The completion of this master's Thesis project would not have been possible without the support, patients, guidance, encouragement, and expertise from two exceptional mentors, Dr. Lisa M. Ellerby and Dr. Swati Naphade.

A debt of gratitude to the Ellerby Lab at the Buck institute for fostering and molding my scientific thinking, as well as the freedom and the support in guiding my scientific curiosity by providing the opportunity to learn as much as the brain can retain.

I have much gratitude for the support team at Dominican University, Dr. Maggie Louie and Dr. Meredith Protas for leading the master's program and keeping us on track. I would like to thank Dr. Robert Barr for taking time to read my thesis.

Last but not least, I would like to thank my parents, Mr. Kumara Silva and Mrs. Sriyani Suwaris, without whom all of this would not have been possible.

Chapter 1

Abstract:

Huntington's disease (HD) is an incurable genetic neurological disorder that affects 1 in 10,000 people, with no treatment that can alter the course of the disease. Neuronal cell death in the striatum and the cortex results from the accumulation of toxic mutant huntingtin protein (mHTT) fragments. Full-length HTT is cleaved by proteases, including caspases, calpains and matrix metalloproteinases (MMP). A multitude of MMP inhibitors have been examined as therapeutic drugs in many diseases including cancer, arthritis, and cardiovascular disease. However, the effects of MMP inhibition in neurodegenerative disorders have not been extensively evaluated. We hypothesize a dysregulation of MMPs and their regulators, tissue inhibitors of matrix metalloproteinases (TIMPs), in the striatum and cortex contribute to the disease pathology of HD, induced by toxic mutant huntingtin fragment formation due to proteolytic cleavage. Thus, investigating the role of MMP inhibition may be a viable route for a HD therapy. Previous research has shown increased levels of MMPs in both human HD post mortem tissue and mouse models, however MMP levels were not studied a HD patient-derived stem cell model. We evaluated MMP expression levels in our HD-patient derived neural stem cell lines by immunocytochemistry and western blot analysis. We found decreased expression levels of MMP-3/10, MMP-14, TIMP-1, and TIMP-2 in our patient derived neural stem cells as well as altered MMP-2 and MMP-9 activity in cells and in secreted media.

Immunocytochemistry further provided evidence of MMP and mutant HTT involvement in HD neural stem cells (NSCs) compared to control corrected NSCs. Further, we evaluated three MMP inhibitor compounds in HD mouse striatal cell line and found these compounds were neuroprotective. To determine if these compounds crossed the BBB and had good pharmacokinetics (PK), we evaluated these compounds in C57BL/6 mice using LC/MS. One MMP inhibitor compound, 9j, showed modest blood brain barrier penetration and specific inhibition of gelatinases (MMP-2 and MMP-9). Overall, our study provided evidence of MMP inhibition is a neuroprotective in mouse striatal cells and one MMP inhibitor compound (9j) crossed the BBB in C57BL/6 mice. However, additional behavioral and biochemical evaluation of 9j needs to be conducted in HD mouse models to provide a better assessment of the beneficial effects of MMP inhibition in HD *in vivo*.

Introduction:

HD is an autosomal dominant neurodegenerative disorder that consumes the later years of life of disease individuals with a triad of symptoms deterring motor ability, cognition, and psychiatric disturbances. These characteristic symptoms of HD are caused by progressive neuronal atrophy and cell death in the cortex and striatum of HD patients, with the GABAergic medium spiny striatal neurons being specifically affected (Huang, Chen, & Zhang, 2016). Current drug treatments merely offer symptomatic benefit for movement disorders and psychiatric and behavioral impairments rather than a cure for the disease. HD pathology arises from polyglutamine (CAG) expansion in the huntingtin (*HTT*) gene which is located on chromosome 4 (Huang et al., 2016; Miller et al., 2010).

Previous research has shown that intracellular HD pathogenesis arises from abnormal aggregation of mutant huntingtin (mHTT) protein, impairments in protein clearance, generation of toxic N-terminal fragments of cleaved truncated mHTT protein, and impaired cellular metabolic pathways (Ross & Tabrizi, 2011). Additional research has shown caspase cleavage of mutant N-terminal HTT to be one driver of neurodegenerative progression in HD (Gafni et al., 2004; Leyva et al., 2010; Schilling et al., 2006a; Wellington et al., 2002c). Differently sized fragments of expressed mHTT found in the striatum suggests progression of disease may be caused by proteolysis of mHTT into fragments cleaved fragments of mHTT (Gafni et al., 2012; Mende-Mueller, Toneff, Hwang, Chesselet, & Hook, 2001; O'Brien et al., 2015; Wellington et al., 2000; Wellington et al., 2002a). Of the various proteases involved in cleaving mHTT, caspases and calpains are most widely studied, however other proteases also have been shown to cleave mHTT, including MMP-10 (Gafni & Ellerby, 2002; Gafni et al., 2012; Hermel et al., 2004). An unbiased siRNA-western blot screen of 514 known human proteases identified 11 proteases that reduced N-terminal toxic fragment formation, three of which belonged to the matrix metalloproteinases (MMP) family, namely, MMP-10, MMP-14, and MMP-23B (Miller et al., 2010). Amino acid deletion experiments were conducted to determine the cleavage of mHtt by MMP-10 to reside at amino acid 402. Proteolysis of mHTT by MMP-10 increases the mutant N-terminal HTT fragments that in turn would cause cytotoxicity. Pharmacological or siRNA knockdown MMP family members decreased cellular toxicity measured by caspase-3/7 activity (Miller et al., 2010). Inhibiting mHTT proteolysis reduced neuronal toxicity suggesting a causal role between

mHTT proteolysis and HD pathogenesis. Our goal was to further investigate the role of MMP inhibition as a potential therapy for HD.

Matrix metalloproteinases are zinc-dependent Ca^{2+} containing endopeptidases that are initially synthesized as zymogens and can be activated by other enzymes or free radicals via a cystine switch. At least 25 human MMP family members have been discovered so far, and they are categorized based on domain structure and substrate specificity (Table 1) (Stefano & Herrero, 2016). MMPs are regulated by other MMP family member as well as their endogenous regulators, tissue inhibitors of matrix metalloproteinases (TIMPs). TIMPs inhibit MMPs by chelating the catalytic Zn^{2+} ion in the MMP catalytic domain. Both MMPs and TIMPs play important roles in several physiological processes, including extracellular matrix remodeling, wound repair, angiogenesis, cell migration, and cell differentiation (Loffek, Schilling, & Franzke, 2011).

Dysregulation of MMPs has been widely implicated in the pathogenesis of several diseases, including cancer, arthritis, and cardiovascular diseases. Recent studies have also shown their involvement in pathogenesis in central nervous system injury and disease (Brkic, Balusu, Libert, & Vandenbroucke, 2015). Dysregulation of MMPs has been linked to various diseases; for example, MMP-3, MMP-1, and MMP-9 upregulation has been linked to rheumatoid arthritis (Araki & Mimura, 2017). Increased MMP-9 CSF levels have been reported in late-stage HD patients and HD transgenic mice (Chang, Wu, Chen, & Chen, 2015; Uchida et al., 2016). Recent literature has also shown that pharmacological inhibition of MMP-9 correlates with reduced neuronal damage and decreased neuronal apoptosis (Hadass et al., 2013). Administration of TIMP-2 has shown

to increase hippocampal function in aged mice (Castellano et al., 2017). The above studies underscore the role of MMPs in maintaining cellular homeostasis, demonstrating that MMP dysregulation can lead to disease pathology.

Because MMP dysfunction is correlated to disease, many therapeutics have been formulated for MMP inhibition (Vandenbroucke & Libert, 2014a). A plethora of MMP inhibitors (MMPi) have been assessed in clinical trials for cancer, arthritis, and cardiovascular disease. Many inhibitors passed phase II and III trials but eventually failed due to drug-induced toxicity as they are broad-spectrum targets of MMPs. MMP genes are highly conserved and essential for cells as they have important regulatory functions in cellular processes such as cell differentiation, migration, survival, apoptosis, growth factor activation, angiogenesis and inflammation (Vandenbroucke & Libert, 2014a). Thus, inhibiting broad range MMPs can cause severe complications. For instance, MMP-1 and MMP-14 inhibition is associated with musculoskeletal disorders.

Due to severe complications and side effects of broad-range MMP inhibitors, chemists have synthesized compounds that is less specific at inhibiting the side-effect causing family members MMP-1 and MMP-14 and specific against a subclass of MMP family members. Thus, *Becker et al.* have synthesized MMP-1 and MMP-14-sparing hydroxamate-based inhibitor compounds (9j, 19v, and 19w) that specifically inhibit MMP-2, -9, and -13 via allosteric inhibition (irreversible). Synthesized compounds (9j, 19v and 19w) were all potent inhibitors that showed efficient inhibition of tumor growth in mice and left-ventricular hypertrophy in rats (Becker et al., 2010). Although these MMP inhibitors have been evaluated in peripheral diseases, the effects of these

compounds have not been evaluated in the context of neurodegenerative diseases and have not been evaluated for BBB penetrance.

Increase in MMP levels have been documented in HD mouse models, post-mortem human brains of HD cells and patients. To better understand how MMPs contribute to HD progression in patients, our lab characterized MMP and TIMP expression in our HD patient (iPSC)-derived HD-NSC line and the CAG-corrected C116-NSC line (An et al., 2012). Our results showed altered expression and localization in MMP-3/10, MMP-14, and activation of MMP-2 and MMP-9 in HD-NSCs compared to corrected C116-NSCs.

We investigated the effects of cellular toxicity in HD mouse striatal cell line Hdh^{111Q/111Q} (disease) and Hdh^{7Q/7Q} (control) treated with MMP inhibitors (9j, 19v, 19w). Rescue of cellular toxicity seen in mouse striatal cells with these MMP inhibitors led us to investigate the efficacy of these compounds in mice (C57BL/6). We evaluated the amount of the MMP inhibitors (9j, 19v, 19w) that penetrated the BBB by performing pharmacokinetic (PK) studies using LC/MS analysis by comparing levels of MMP inhibitors (9j, 19v, 19w) in the brain relative to plasma levels. Lastly, we evaluated the specificity of MMP inhibition utilizing gelatin zymography and enzymatic assays using a fluorogenic substrate (Mac-Pro-Leu-Ala-Nva-Dap (Dnp)-Ala-Arg-NH₂). With the observed changes in MMP and TIMP expression via immunoblotting techniques along with low levels of cytotoxicity seen by caspase-3/7 assay in HD mouse striatal cell line, we extended our investigation/evaluation of MMP inhibitors (9j, 19v, 19w) in mice (C57BL/6). Even with modest amount of compound detected in the brain we did see

specific inhibition of gelatinases in brain lysates via gelatin zymography and enzymatic assay analysis.

Methods:

Cell Culture

To generate C116-iPSC and HD-iPSC lines we used STEMdiff Neural Induction Medium using the protocol from (Ring et al., 2015) and characterized these cells as previously done in lab (An et al., 2012). Matrigel was used to coat 60 mm dishes for one hour before cells were plated and cultured in Neural Proliferation Medium (NPM) in a humidified incubator under 37°C, 5% CO₂. Neurobasal medium with 1X B-27 supplement (2mM L-Glutamine, 100U/mL penicillin, 100 µg/mL streptomycin, 10 ng/mL human Leukemia Inhibitory Factor (LIF) (Peprotech, 300-05), and 25 ng/mL human basic Fibroblast Growth Factor (bFGF) (Peprotech, 100-18B) was used to prepare the NPM.

Western Blot Analysis

Neural stem cells were lysed with lysis buffer (M-PER + Roche complete protease inhibitor). Lysates were sonicated for 5 x 5 second pulses at 40 mA. Samples then were centrifuged at 14,000 rpm at 4°C and the supernatant collected for western blot analysis. Protein concentration was measured using a BCA assay (Pierce). 10 – 20µg of total protein lysate was added to 4X LDS sample buffer (Invitrogen) and 1µl of 1M DTT and then boiled for 10 minutes at 95°C. SDS-PAGE was performed using a 4% – 12% NuPAGE Bis-Tris gel (Invitrogen). Gels were run at 200V for 55 minutes in MES (Invitrogen) running buffer, then transferred to PVDF membrane in 1X NuPage transfer buffer overnight at 20V at 4°C. Membranes were then blocked in TBS with 0.1% Tween

20 (TBS-T) and 5 % non-fat milk for one hour. Primary antibodies were reconstituted in 5% non-fat milk in 1X TBS-T and then probed overnight at 4°C, followed by incubation with secondary antibody for 3 hours at room temperature. Lastly the membranes were washed (3X) for 10 minutes, developed using Pierce ECL (Thermo Scientific), and band intensity was quantified by ImageQuant. α -tubulin and β -actin were used as controls. Basal levels of MMP and TIMP expression were measured in HD-NSCs and C116-NSCs. MMP levels were measured post administration of MMP inhibitor compounds. Concentrations of primary antibodies used were: MMP-9 (1:100), MMP-2 (1:100), MMP-3/10 (1:250), TIMP-1 and TIMP-2 (1:250).

Immunocytochemistry

Cells were cultured in 8-well chamber slides (BD Falcon) and fixed in 4% paraformaldehyde in PBS for 15 minutes at room temperature. Cells were washed 2X with PBS and blocked for 30 minutes at room temperature with blocking buffer (0.1% TritonX-100, 5% Donkey Serum, PBS), and then incubated with primary antibody (suspended in 5% donkey serum in 1% BSA in 1X PBS) at 4°C overnight. The following day, slides were washed 3X for 10 minutes and blocked with secondary fluorescently conjugated antibody (1:200 suspended in 1% BSA in PBS) for 1.5 hours at room temperature. Slides were washed 3x for 10 minutes with PBS. Lastly, a coverslip was mounted with ProLong Gold with DAPI (1:500 suspended in PBS) and cured for 24 hours at room temperature. Primary antibodies used were: MMP-14 (1:50), MMP-2 (1:50), MMP-9 (1:50), MMP-3 (1:50), MMP-10 (1:50). Imaging was performed on the Nikon Eclipse Ti-U microscope.

Caspase-3/7 Assay

The caspase activity assay was performed with Apo3 HTS kit (Cell Technology). Hdh^{111Q/111Q} and Hdh^{7Q/7Q} mouse striatal cells were cultured in collagen I coated 96-well plates (BD) in serum free media (1X DMEM) along with MMP inhibitor compound (9j, 19v, and 19w) for 24 hours. Medium was removed and 50 µl of caspase assay lysis buffer (50% Apo3 HTS lysis buffer/50% PBS) was added into each well. After shaking on an orbital shaker at 700 rpm for 5 minutes, two 10 µl aliquots of lysate were transferred to new 96 well plates for protein quantification by BCA protein assay (Thermo Scientific). To the remaining 30µl of cell lysate, 70 µl of substrate mix (1X Apo3 HTS Caspase-3/7 detection reagent) and 1 M DTT were added to each well. The plate was shaken at 700 rpm for 30 seconds before reading. The Victor3X spectrophotometer (Perkin Elmer) was used for this fluorescence-based assay (Ex: 485nm, Em: 530nm) at 37°C. The caspase activity was normalized against protein concentration of each sample.

Pharmacokinetic Mouse Study

A single dose of 25 mg/kg body weight of MMP inhibitor: 9j (10% EtOH), 19v (10% EtOH), and 19 (10% EtOH) was injected into the intraperitoneal cavity of the 5-6-week-old C57BL/6 mice (Jackson labs). Twenty one female mice were used for each inhibitor compound tested (n = 3 for 0.5, 1, 2, 4, 8 hours.). At each subsequent time point, 200 µl of blood was collected from a retro-orbital bleed under controlled isoflurane anesthesia. Blood was immediately transferred to heparinized tubes (BD) on ice, tubes were spun at 8500 rpm at 4°C for 10 minutes, and plasma was separated into separate tubes for LC-MS analysis. Following blood collection, the mouse was sacrificed, the brain was

harvested, and split into right and left hemispheres, and weights of the individual hemispheres were recorded. One hemisphere was sent for LC/MS analysis (Integrated Analytical Solutions Inc.), and the other half was used for gelatin zymography and enzymatic assay analysis. Analysis of the compounds in plasma and brain at each time point was conducted by Integrated Analytical Solutions, Inc.

Gelatin Zymography

The right halves of the compound administered mouse brains at each time point were homogenized with lysis buffer (50mM Tris-HCL, 150mM NaCl, 5mM CaCl₂, 0.05% Brij-35, 1% Triton X-100, 0.02% NaN₃), sonicated 3x for 30 seconds, left for 30 seconds of rest at 40% amplitude and centrifuged at 14,000 rpm for 20 minutes at 4°C. For HD-NSCs and C116-NSCs, cells were homogenized in the same lysis buffer and sonicated for 5 x 5 seconds at 40% amplitude. Following protein determination via BCA assay (Pierce), tissue (500 µg) and cell (50 µg) whole lysate was incubated with 50 µg of gelatin Sepharose 4B beads (GE healthcare) on a rotator at 4°C for one hour for MMP binding. The suspension was centrifuged, the supernatant discarded, and affinity-bound MMP was eluted with 50 µl of 10% DMSO on a rotator at 4°C for one hour. Affinity-purified MMPs in 1 x LDS dye were then loaded onto 1% gelatin infused 10% SDS-PAGE at 90V for 15 minutes, then increased to 150V for 90 minutes. Afterwards, gels were incubated with 2% Triton X-100 in water for 30 minutes at room temperature, washed 3X with ddH₂O, and incubated in developing buffer (50mM Tris, 5mM CaCl₂, 200mM NaCl, 0.02% Brij-35) for 72 hours at 37°C. Following 72 hour incubation, gels were stained with 0.5% Coomassie blue (10% acetic acid, 50% methanol) for one hour

and destained (40% methanol, 10% Acetic acid, 50% ddH₂O) for another hour at room temperature. Lastly, EPSON image scan was used to scan the gels.

Enzymatic Assay

Brain tissues of mice obtained at each timepoint were homogenized in lysis buffer (50 mM Tris-HCL, 150 mM NaCl, 5 mM CaCl₂, 0.05% Brij-35, 1% TritonX-100, 0.02% NaN₃), sonicated 3X for 30 seconds with 30 seconds of rest at 40% amplitude and centrifuged at 14,000 rpm for 20 minutes at 4°C. BCA assay (Pierce) was performed to determine the protein concentration. 140 µg of protein, 7.5 µM of NNGH, 4µM of fluorogenic substrate, Mac-Pro-Leu-Ala-Nva-Dap (Dnp)-Ala-Arg-NH₂ (Enzo labs), and assay buffer (50mM HEPES, 10mM CaCl₂, 0.05 % Brij-35, pH 7.5) was loaded onto a 96 well black-bottom plate. Substrate fluorescence intensity was measured (Ex: 485nm, Em: 530nm) at 37°C by VictorX3 (Perkin Elmer). The enzymatic activity was normalized to protein concentration of each sample. Fluorescence readings were provided by Workout Plus software. Fluorescent readings of the drug-induced lysates were compared to the addition of NNGH, a broad spectrum MMP inhibitor, to measure the overall activity of MMP-2 and MMP-9.

Results:

Altered MMP-3/10 and MMP-14 Expression in HD-NSCs vs. C116-NSCs

Previous studies have shown dysregulated levels of MMP-14 and cleaved MMP-10 in the Hdh^{111Q/111Q} HD mouse striatal line, compared to the Hdh^{7Q/7Q} control line (Miller et al., 2010). Thus, we looked at the corrected C116-NSC line via immunocytochemistry and western blot analysis. We found a 1.6-fold increase in MMP-

3/10 expression between the HD-NSCs and the C116-NSCs (**Fig. 1A**). Antibody staining shows an altered localization of MMP-3/10; it is cytosolic in C116-NSCs and has an increased nuclear localization in HD-NSCs. High expression of MMP-3/10 is observed in degenerated nuclei of apoptotic cells identified by merging DAPI staining and amplified fluorescent signaling of MMP-3/10 (white arrows) (**Fig. 1B**). MMP-14 expression levels were decreased by 1.7 fold in HD-NSCs compared to C116-NSCs as shown by western blot analysis, (**Fig. 2A**). Both MMP-14 and HTT antibody staining show nuclear localization in HD-NSCs compared to C116-NSCs (**Fig. 2B**).

Gelatinase (MMP-2 and MMP-9) Expression and Activity in NSCs

Dysregulation of MMP-2 and MMP-9 have been implicated in the progression of various disease pathologies. Increase in neuroinflammatory markers, one of which is MMP-9, have been observed in HD patients and HD mouse models (Chang et al., 2015). We looked at the expression, cellular localization, and activity to measure whether these characteristics are displayed in our HD-patient derived NSCs. Activity of MMP-2 and MMP-9 were determined using gelatin zymography in whole cell lysates of HD-NSCs as well as the secreted gelatinase activity in the conditioned media (**Fig. 3A and B**). We visually observed a decrease in MMP-2 activity and an increase in the proform of MMP-9 in whole cells as well as in the secreted media. Immunocytochemistry further demonstrates MMP-2 expression is increased in C116-NSCs compared to HD-NSCs (**Fig. 3C**). We also observed that MMP-2 expression aligned with apoptotic cells in both C116-NSCs as well as HD-NSCs (**Fig. 3C**). We also observed increased nuclear expression of gelatinases in HD-NSCs (**Fig. 3C-D**).

Altered TIMP Expression in HD-NSCs and C116-NSCs

Tissue inhibitors of Matrix Metalloproteinases (TIMPs) are endogenous inhibitors of MMPs and previous research has shown elevated TIMP levels in the cerebrospinal fluid in post-mortem brains of patients with neurodegenerative diseases, such as Alzheimer's Disease (AD), Parkinson's Disease (PD), ALS, and HD (Lorenzl et al., 2003). We evaluated whether the levels of TIMPs were modulated in our NSCs. We found that TIMP-1 [Fig. 4A (3.3-fold decrease)] and TIMP-2 [Fig. 4B (1.6-fold decrease)] expression was downregulated in HD-NSCs compared to the CAG corrected C116-NSC line. We confirmed by immunocytochemistry that the expression of TIMP-1 is decreased in HD-NSCs while the expression levels of HTT aggregates are increased when compared to C116-NSCs (Fig. 4C).

MMP Inhibitors Reduce Cellular Toxicity in HD Mouse Striatal Cell Line.

We measured, *in vitro*, the cellular toxicity in HD mouse striatal cells in response to the treatment of MMP inhibitor compounds (9j, 19v, and 19w). Our experiment measured caspase-3/7 activity in stressed serum deprived striatal cells with (Hdh^{111Q/111Q}) and without (Hdh^{7Q/7Q}) CAG expansion. No significant change in the levels of caspase-3/7 activity was detected in the control striatal cell line (Hdh^{7Q/7Q}) between the treated and non-treated cells. However, we did see a significant reduction in caspase-3/7 activity in the HD striatal cell line (Hdh^{111Q/111Q}) with 10 μ M treatment of MMP inhibitor compound. All three compounds showed a reduction in caspase-3/7 activity between the treated and non-treated Hdh^{111Q/111Q} cells: 9j, 25% reduction in caspase-3/7 activity (Fig. 5A); with a $p < 0.001$, 19v, 30% reduction (Fig. 5B); with a $p < 0.001$, and 19w, 37% reduction (Fig. 5C); with $p < 0.01$.

Pharmacokinetic Study of MMP Inhibitor Compounds in Mice

MMP inhibitors have been investigated as therapeutic drugs for many peripheral diseases. Most have failed Phase 1 clinical trials due to complication of broad-spectrum MMP inhibition. We tested three MMP inhibitor compounds (**Table 2**) that were synthesized by *Becker et.al* group to have MMP-1 sparing ability as well as high specificity of inhibition towards gelatinases, MMP-2 and MMP-9 (Becker et al., 2010). Initial pharmacokinetic study was performed using C57/BL6 mice to evaluate the compound that best penetrated the BBB. Mice were given a single IP injection of 25mg/kg body weight of MMP inhibitor compound (9j, 19v, and/or 19w), sacrificed at 0.5, 1, 2, 4, and 8 hours post-dosing (n = 3 mice per time point) and the brain and plasma levels were analyzed by LC/MS-MS: 9j compound (**Fig. 6A**), 19v compound (**Fig. 6B**), and 19w (**Fig. 6C**). MMP inhibitor compounds were detected at an average of 5 µg/ml for 9j, 12 µg/ml for 19v, and 36 µg/ml for 19w in blood plasma at 30 minutes post initial administration. A comparison of the MMP inhibitor compounds in brain tissue relative to amounts detected in plasma showed an increase in >5% in all compound, except for 9j (**Fig. 6D**), however no statistical significance was found. We calculated the brain tissue to plasma ratio of each compound at each time point. Percentage of the compound that penetrated the brain from total amount in plasma was compared at each timepoint for the 9j, 19v, and 19w administered mice. No statistical significance was found in compound retained in brain tissue relative to amounts in the plasma at any point post administration. There was also no significance of the compound retention percentage in brain tissue when compared between each of the MMP inhibitors except at the eight-hour time point. We observed a 20% increase of the 9j compound in brain tissue was detected in comparison 19v and 19w retention levels (2-way ANOVA, Tukey's multiple test, $p < 0.001$) (**Fig. 6D**). MMP

inhibitor compound 9j seems to be the best inhibitor compound, of those tested, in penetrating the BBB as measurement of the ratio comparing the relative amount of compound in brain tissue to the levels in blood plasma.

Gelatinase (MMP-2 and MMP-9) Inhibition in Brain Tissue Lysates of MMP Inhibitor Compound Administered Mice

We saw modest amounts of MMP inhibitor compound retention in the brain tissue of mice, but 9j was seen to have better tissue retention compared to the other two compounds. Thus, as a further step, we wanted to confirm the specificity of gelatinase inhibition in 9j administered mice at each time point. To this end we conducted gelatin zymography to visualize and detect active MMP-2 and MMP-9 in the brain lysates of MMP inhibitor treated mice. Gelatin zymogram of 9j compound brain lysates (n = 3 mice) shows greater MMP-9 and MMP-2 activity, measured by gelatin degradation, at 30 minutes compared to low to no activity of MMP-9 and MMP-2 at the 4 hour timepoint post-administration (**Fig. 7A**). MMP-2 and MMP-9 activity is also reduced at 1 hour and 2 hour post-injection (**Fig. 9**). Furthermore, quantification of MMP-2 activity of brain lysates measured by enzymatic assay using a fluorogenic substrate shows a reduction in MMP-2 activity at 2 hour and 8 hour timepoints (Tukey's multiple test, $p < 0.02$) (**Fig. 8A**). Activity of MMP-2 and MMP-9 was lowered with the administration of MMP inhibitor compounds while the expression level of MMP-2 detected by western blot analysis remained unaltered (**Fig. 9**) and the expression of MMP-9 increased at a 2 hour timepoint (One-way ANOVA, Dunnett's multiple comparison test, $p < 0.02$) and decreased at an eight-hour timepoint (One-way ANOVA, Dunnett's multiple comparison, $p < 0.01$) (**Fig. 9**).

We also looked at gelatinase activity in mice treated with 19v and 19w MMP inhibitor compounds. Gelatinase activity of MMP-2 increased at the 1 hour timepoint and then activity level decreased at the later 1 hour timepoint when compared to the vehicle-administered control (**Fig. 7B**). Quantification of MMP-2 enzymatic activity (**Fig. 8B**) detected with the cleavage of fluorogenic substrate did not show any statistical significance at any timepoint, nor did the expression of MMP-9 change as detected by western blot (**Fig. 10C**). Gelatinase activity of 19w compound showed little MMP-9 activity for all timepoints and high MMP-2 activity at the 30 minutes and later reduced at the last 8 hour (**Fig. 7C** and **9C**). Quantification of MMP-2 enzymatic activity assay shows no statistical significance in activity between the timepoints to the non-administered control (**Fig. 8C**). Western blot analysis shows unaltered expression of MMP-2 (**Fig. 10D**) for all timepoints when compared to non-treated control. MMP-9 (**Fig. 11D**) expression is not statistically significant except for decrease in expression between four-hour and eight-hour timepoint (One-way ANOVA, Tukey's multiple comparison test, $p < 0.02$).

Discussion:

No treatment is currently available to slow the progression of Huntington's disease. Many of the therapeutics available are to alleviate the symptoms resulting from the disease. HD pathogenesis leads to neuronal death which is caused by toxic Htt fragments formed by the proteolysis of mHtt (Mende-Mueller et al., 2001; Wellington et al., 2002b). A previous study has shown that proteases other than calpains and caspases cleave mHtt, specifically MMP-10 (Miller et al., 2010). Studies conducted in the field have detected increase in MMP levels in the cerebrospinal fluid of HD patients as well as brain tissue of

HD mice (Chang et al., 2015; Connolly et al., 2016). Our main aim was to investigate MMPs as a therapeutic target for HD, in that by reducing or inhibiting MMPs we can modulate the proteolysis of mHTT that can confer neuroprotection via the reduction of the toxic N-terminal HTT fragments.

We can see a dysregulation of certain MMPs in our HD-patient derived NSC line when compared to the CAG-corrected C116-NSC line. Previous research showed MMP-10 cleavage of N-terminal mHTT. However, all MMPs share sequence similarities; MMP-3 and MMP-10 are both classified as stromelysin (**Table 1**) and show an 86% similarity of the catalytic domain (Bertini et al., 2004). MMP-3 has the ability to cleave mHtt, similar to MMP-10 (unpublished data). To this end we compared the expression of MMP-3/10 in our NSC line and found a significant increase (**Fig. 1A**) between the HD and control corrected line as well as high nuclear localization in HD-NSCs compared to C116 (**Fig. 1B**). Furthermore, we also see a nuclear presence of HTT aggregate formation in degenerating nucleus of the HD-NSCs (**Fig. 2B**), which leads us to speculate that MMP-3 and MMP-10 might interact with mHTT. It is unclear whether other members of the MMP family contribute to cytotoxicity. This further provides the basis to investigate MMP inhibition as a possible therapeutic target to combat cellular toxicity caused by mHtt proteolysis.

We found that the expression of MMP-14 is lower in HD-NSCs compared to C116 (**Fig. 2**), which contradicts previous findings that showed an increase in MMP-14 levels in HD mouse striatal cell line (Miller et al., 2010). These differences can be attributed to gene expression variation between mouse and human cell lines. Differences can also result from one being a fully differentiated striatal cell line and a multipotent NSC line.

However, upregulation of MMP-14 have been reported in brain regions with high amyloid pathology of AD patients as well as elevated MMP-14 levels near reactive astrocytes containing degraded A β deposits (Liao & Van Nostrand, 2010). We can speculate that the up-regulation of MMP-14 seen in the AD model to take a protective role in clearing A β aggregates. This MMP-14 up-regulation model may have the same role in clearing mHtt aggregates in HD, which is observed to be elevated in the differentiated striatal cell that is less prone to stress compared to the pluripotent NSC line. To validate possible increase in MMP-14 and mHTT clearance ability we need to further differentiate our HD-NSCs into striatal cells and measure the levels of MMP-14 as well as the levels of mHTT fragments.

We also observed decreased levels of activated MMP-2 and increased levels of activated MMP-9 in both the cellular lysates (**Fig. 3A**) and the conditioned media (**Fig. 3B**) of HD-NSCs. Activation of MMP-2 requires forming a tetrameric proMMP-2 activation complex involving MMP-14, TIMP-2 and MMP-2 (Li et al., 2017; Nagase, Visse, & Murphy, 2006). Decreased expression of MMP-14 (**Fig. 2**), and TIMP-2 (**Fig. 4B**) in HD-NSCs provides basis for the reduced activation of MMP-2 (**Fig. 3A-B**) seen by the gelatin zymography. Immunocytochemistry analysis showed an increase in nuclear expression of both MMP-2 and MMP-9 in degenerating nuclei (**Fig. 3C**). Many cellular processes have been associated with MMP-2 and MMP-9 regulation. Nuclear expression of MMP-2 has been associated with initiation of the apoptotic pathway through the inactivation of poly-ADP-ribose-polymerase-1(PARP-1) (Kwan et al., 2004). Increase in nuclear expression of MMP-2 and MMP-9 in degenerating nuclei correlates to initiation of the apoptotic pathway in highly stressed NSCs. Determining the role of MMP-9 in

neurodegenerative disease has been confounding in that MMP-9 has shown to be neuroprotective in AD due to its ability to degrade A β (Mizoguchi et al., 2009) and knockout of MMP-9 was shown to correlate with an increase in number of functional dopaminergic neurons in models of PD (Annese et al., 2015). Over all, the consensus on the significance of MMP-9 in neurodegenerative disease is that the increased expression in cerebrospinal fluid is a potential biomarker and possibly a therapeutic target for neurodegenerative disease, such as AD, PD, and HD (Vafadari, Salamian, & Kaczmarek, 2016).

Western blot analysis shows a decrease in TIMP-1 and TIMP-2 expression in HD-NSCs compared to C116-NSCs (**Fig. 4A-B**). TIMPs are endogenous inhibitors of MMPs and altered MMP:TIMP ratios have been investigated in neurodegenerative diseases where elevated levels of TIMPs in CSF have been found in AD, PD, HD and ALS patients (Lorenzl et al., 2003). TIMP-1 may function to protect against the MMP-mediated expansion of neuroinflammatory markers induced by MMP-9 (Crocker, Pagenstecher, & Campbell, 2004). Immunocytochemistry analysis further confirms the lower levels of TIMP-1 expression in HD-NSCs (**Fig. 4C**). We also see co-localization of TIMP-1 and mHtt in aggregate structure surrounding HD-NSCs. This leads us to speculate that TIMP-1 inhibits MMP-10, which has been previous shown to cleave mHTT (Miller et al., 2010). The dysregulation presented by an increase in MMP-10 expression and a decrease in TIMP-1 expression proves that HD-NSCs are prone to more stress due to the inability of TIMP-1 to regulate MMP-10 proteolysis which leads to mHTT fragment accumulation. This leads us to consider that pharmacological inhibition of MMPs is a

viable therapeutic strategy to reduce the cytotoxicity induced by mHTT fragment accumulation.

MMP inhibitor compounds have been evaluated in various peripheral diseases, however phase III clinical trials have been highly unsuccessful, due to the difficulty of formulating a MMP inhibitor compound that can specifically target one family member, as MMP family members are highly conserved in their protein structure (Bertini et al., 2004). Becker *et. al.* group formulated a few compounds that specifically inhibited MMP-2, MMP-9 and MMP-13 while sparing MMP-1 and membrane-bound MMP-14 through hydroxamate-based inhibition. Hydroxamate-based inhibitors bind to the Zn^{2+} and distort the geometry around the Zn^{2+} ion, reducing the enzyme's Zn^{2+} binding ability (Vandenbroucke & Libert, 2014b). Metalloproteinase selectivity was achieved by exploiting the size difference of the S1' subunit which created a steric blockade of the binding site (Becker et al., 2010). MMP inhibition was conducted in blood plasma of rats and the activity of MMP-2 and MMP-9 at IC_{50} value was < 0.1 and the bioavailability was $> 20\%$ for each compound (**Table 2**).

We initially tested these three inhibitor compounds in HD mouse striatal cell lines and found them to be neuroprotective. Previous research showed that wild type HTT protein protects cells from apoptosis upstream of caspase-3 (Rigamonti et al., 2000), while huntingtin with expanded polyglutamine undergoes cell death (Conforti et al., 2013). Our caspase-3/7 enzymatic assay measured the levels of fluorogenic substrate cleaved by activated the caspase-3/7 thus providing evidence of cells undergoing cell death. All three MMP inhibitor compounds were found to be neuroprotective in that treated HD cells had lowered caspase-3/7 activity compared to no difference in wild type mouse striatal cells

(**Fig. 5**). As these compounds were neuroprotective in mouse striatal cells, we evaluated these compounds in mice.

The compounds were selected based on properties that would predict they might cross the BBB. However, whether this was the case required a careful analysis of PK in mice. We evaluated these three compounds in C57/BL6 mice via a pharmacokinetic study coupled to LC/MS. 19w compound were detected at higher amounts in both the plasma and brain tissue at 30 minute timepoint compared to 19v and 9j. The amounts of MMP inhibitor compounds decreased in respective to time, but only 9j compound showed a close convergence of the plasma concentration curve and brain tissue concentration curve (**Fig. 6A**). The amount of inhibitor compound detected in the brain tissue was less than five percent of the compound concentration detected in the blood plasma at each of the timepoint. Comparison of the percent compound concentration (amount of compound in brain relative to plasma levels) between each of the MMP inhibitors did not show any one compound to be better at penetrating the blood brain barrier at the first four timepoints. However, a comparison of the compound retained in the brain tissue in comparison to the levels in blood plasma at the last timepoint showed a significant increase in 9j inhibitor compound compared 19v or 19w (**Fig. 6D**), this might be due to its smaller molecular weight and low cLogP value, which is a measure of compounds hydrophilicity (**Table 2**). 9j compound has a smaller molecular weight and a lower partition coefficient then other two compounds, 19v and 19w, two characteristics that would allow for good permeation of a compound. We tested the compounds in wild type mice to measure the overall ability of these compounds to cross the BBB. While there was a modest retention of MMPi compound in the wild type mice we believe that in R6/2

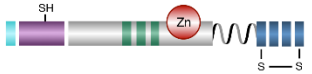
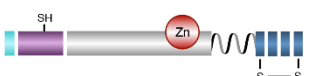
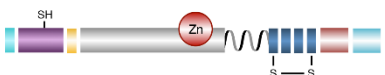

mice, where the BBB is highly compromised (Drouin-Ouellet et al., 2015), more MMP inhibitor compound would be retained.

Next, we wanted to test the specificity of MMP-2 and MMP-9 of each inhibitor compound via gelatin zymography and enzymatic assay with fluorescent substrate. No activity of MMP-2 was visually visible in the gelatin zymograms at the last timepoint of 9j, 19v, and 19w administered mice (**Fig. 7A-C** and **Fig. 9**) when compared to 30 minutes post injection which visually confirms the specificity of MMP inhibition on MMP-2. MMP-2 specific enzymatic assay performed on 19v (**Fig. 8B**) and 19w (**Fig. 8C**) showed no statistical significant in the reduction of MMP-2 enzymatic activity when compared to non-treated mice. We did see a difference in MMP-2 activity at 2 hour and 8 hour time points in 9j administered (**Fig. 8A**) brain lysates which was visually displayed by gelatin zymograms (**Fig. 9**) at the corresponding time point. We did not see any altered protein expression of MMP-2 (**Fig. 10B-C**) and MMP-9 (**Fig. 11B-C**) as quantified by western blot analysis for 19v and 19w. Interestingly for 9j administered brain lysates no change in MMP-2 expression was noted (**Fig. 10A**), but a significant difference in MMP-9 expression (**Fig. 11A**) at the corresponding time point (two and eight-hour) when compared to non-MMP inhibitor treated mice. Increase in MMP-9 expression at the 2 hour timepoint might be due to a compensatory effect in the brain as a result of MMP-2 inhibition as both MMP-2 and MMP-9 are in the same subclass of MMP family member, gelatinases.

In conclusion, we found dysregulation of certain MMP family member in our patient derived HD-NSC model. This dysregulation likely leads to proteolysis of mHTT and to neuronal cell death. Thus, inhibition of proteases that cleave mHTT may be

neuroprotective. MMP inhibitor compounds tested in mouse striatal cells were shown to be neuroprotective as measured by caspase-3/7 activity. Our pharmacokinetic study of MMP inhibitor compounds showed that 9j had a better retention in brain tissue at the end time point compared to 19v and 19w. MMP inhibitor 9j also showed good specificity towards inhibiting MMP-2. We would like to start a treatment with the 9j MMP inhibitor compound to evaluate the benefit of MMP inhibition on locomotor decline in R6/2 mice.

Tables and Figures:

	Name	Location	Main substrates / Proteases inhibited*	Structure
MMP-2	Gelatinase A	Secreted	ECM: collagens, gelatin, elastin, fibronectin, etc. Non-ECM: pro-IL-1b, plasminogen, other MMPs	
MMP-9	Gelatinase B	Secreted		
MMP-3	Stromelysin-1	Secreted	ECM: collagens, gelatin, elastin, fibronectin, laminin, aggrecan Non-ECM: pro-IL-1b, plasminogen, pro-MMP-1, -8, -9, -13, MMP/TIMP complex, antithrombin III, fibrinogen, plasminogen, IGFBP	
MMP-10	Stromelysin-2	Secreted		
MMP-14	Transmembrane type 1 MMP	Membrane-bound	ECM: collagens, gelatin, elastin, laminin, vitronectin Non-ECM: pro-MMP-2 and -13	
TIMP-1	-	Secreted	Inhibits all MMPs, except MMP-14	
TIMP-2	-	Secreted	Inhibits all MMPs tested, required for pro-MMP-2 activation	













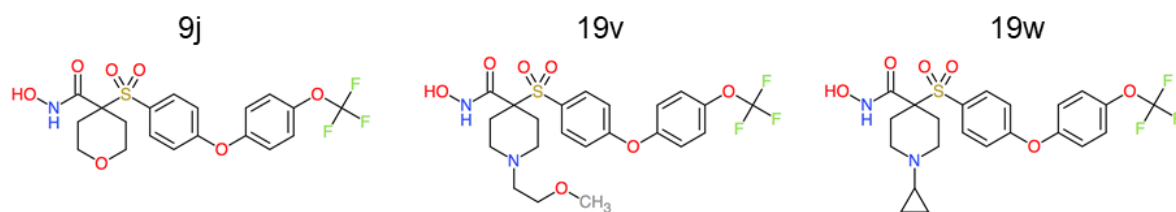
 Signal peptide	 Fibronectin domain	 Zinc cation	 Furin domain
 Pro-peptide	 Hinge region	 Transmembrane domain	 N-terminal
 Catalytic domain	 Hemopexin domain	 Cytoplasmic domain	 C-terminal

Table 1: Structure and Classification of MMPs and TIMPs

Courtesy of *Frontiers in Neuroscience* journal originally appeared in (Naphade, Embusch, Madushani, Ring, & Ellerby, 2018)



Compound	Class	Mol. Wt.	MMP-1	MMP-2	MMP-3	MMP-7	MMP-8	MMP-9	MMP-13	MT1-MMP	clogP	C _{max} (ng/mL)	C _{6h} (ng/mL)	t _{1/2} (h)	BA (%)
9j	α-Tetrahydropyranyl Sulfones	461.07	1140	<0.1	35	1140	0.9	0.2	<0.1	10.6	1.83	8584	1172	1.87	35.9
19v	α-Piperidine Sulfones	572.12	>10K	<0.1	28.7	7000	1.7	0.18	<0.1	13	2.44	29634	20521	2.94	67.9
19w	α-Piperidine Sulfones	536.09	4000	<0.1	22	7000	1.2	0.15	0.1	4.6	2.58	4160	440	2.58	23

Table 2: Structure and PK Parameters of MMP Inhibitor Compounds

Chemical structure of the MMP inhibitor compounds; 9j, 19v, and 19w. PK parameter's and MMP activity at IC₅₀ values are courtesy of Journal of Medicinal Chemistry. Table has been adapted from (*Becker et al., 2010*)

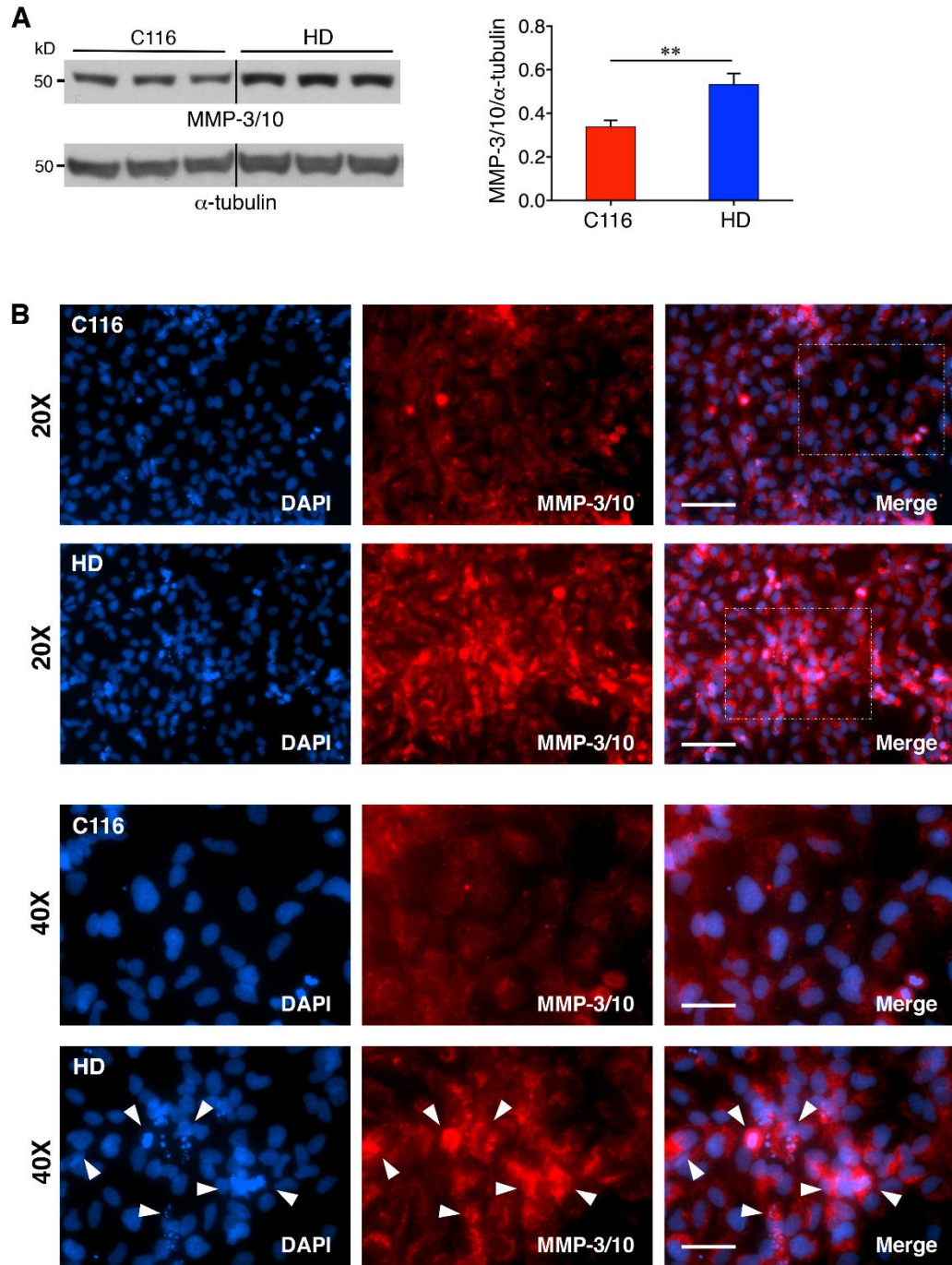


Figure 1: Increased Expression of MMP-3/10 in HD-NSCs

- (A) Western Blot analysis of MMP-3/10 shows increase in expression in HD-NSCs and quantification when compared to α -tubulin shows a significant increase evaluated by student t-test ($n = 3$ biological replicates, $**p < 0.01$).
- (B) Immunofluorescence analysis shows increase in MMP-3/10 in HD-NSCs compared to C116-NSCs. Increased presence of MMP-3/10 in apoptotic cells as shown by white arrows. (scale bar: 20X = 100 μ m and 40X = 50 μ m). Originally appeared in (Naphade et al., 2018).

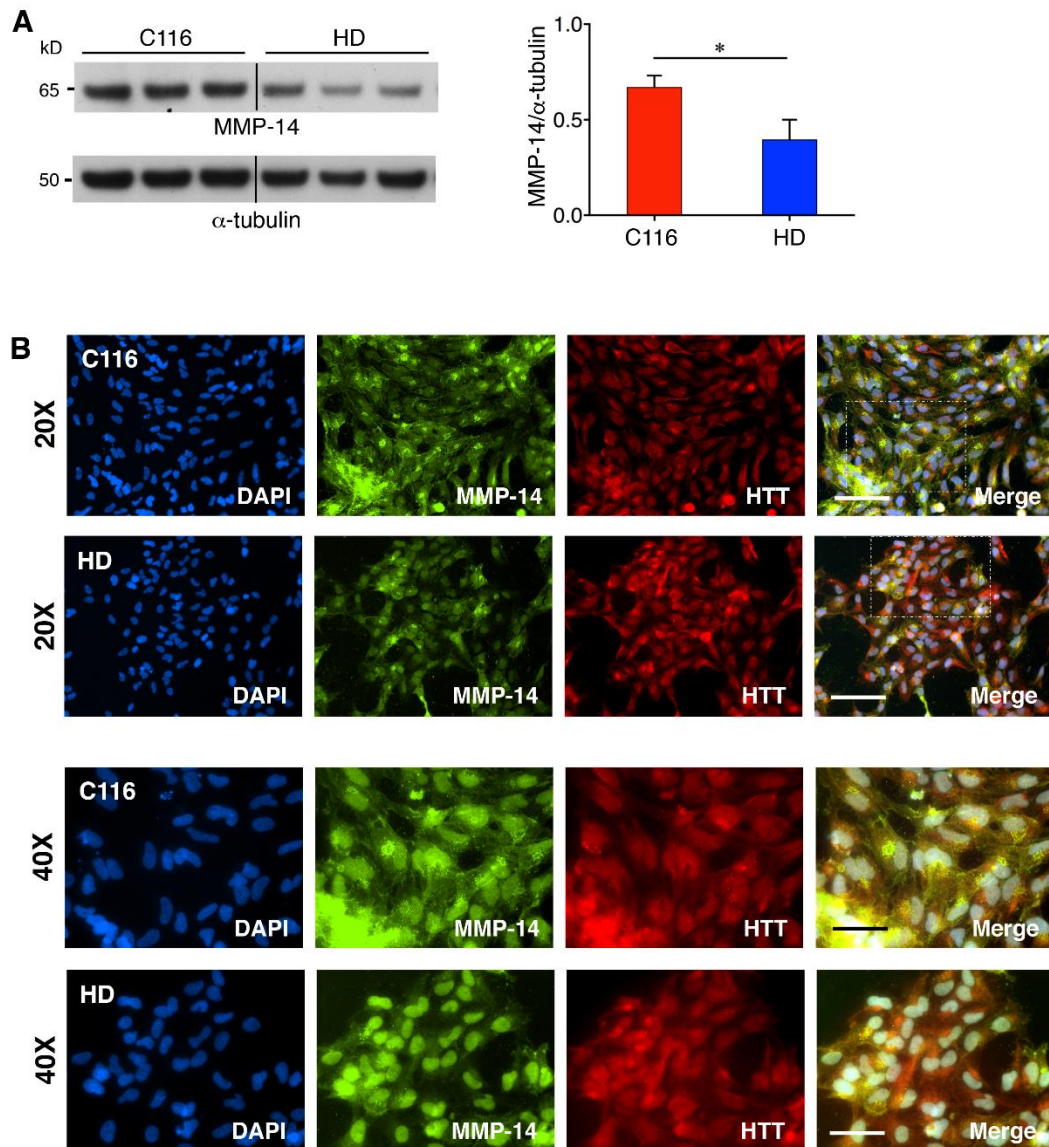


Figure 2: Decreased Expression of MMP-14 in HD-NSCs

- (A) Western blot analysis of MMP-14 expression in HD-NSCs. Quantification of MMP-14 expression compared to α -tubulin shows a significance ($*p < 0.05$) reduction in MMP-14 expression in HD-NSCs.
- (B) Immunocytochemistry analysis shows decreased expression in HD-NSCs and higher expression of HTT expression. MMP-14 expression in HD-NSCs is predominantly nuclear compared to C116-NSCs where HTT expression is also observed in the cytoplasm. (Scale bar 20X = 100 μ m: 40X = 50 μ m) Originally appeared in (Naphade et al., 2018).

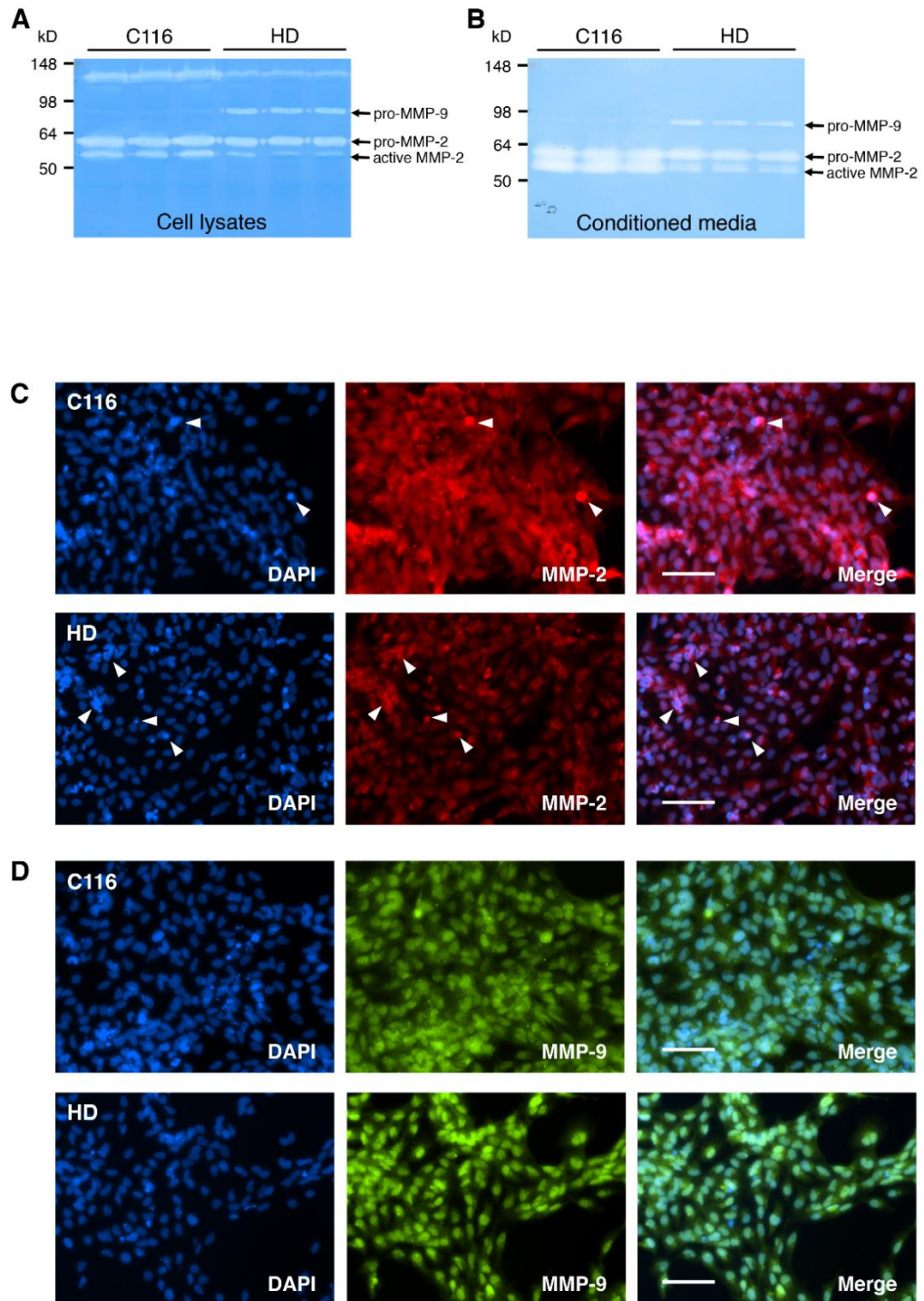


Figure 3: Altered MMP-2 and MMP-9 Activity and Localization in HD-NSCs

- (A) Gelatin zymography shows decreased activity of MMP-2 and higher activity of MMP-9 in cell lysates of HD-NSCs compared to C116-NSCs.
- (B) Gelatin Zymography shows the same decreased activity of MMP-2 and increase in activity of MMP-9 in conditioned media of HD-NSCs compared to C116-NSCs.
- (C) Immunocytochemistry show increase in MMP-2 expression in C116-NSCs and an increased expression of MMP-2 of degenerating nuclei in both HD-NSCs and C116-NSCs indicated by the white arrows. (scale bar: 20X = 100 μ m)
- (D) Immunocytochemistry analysis of MMP-9 in HD-NSCs shows an increased nuclear expression in HD-NSCs compared to C116-NSCs. (scale bar: 20X = 100 μ m). Originally appeared in (Naphade et al., 2018).

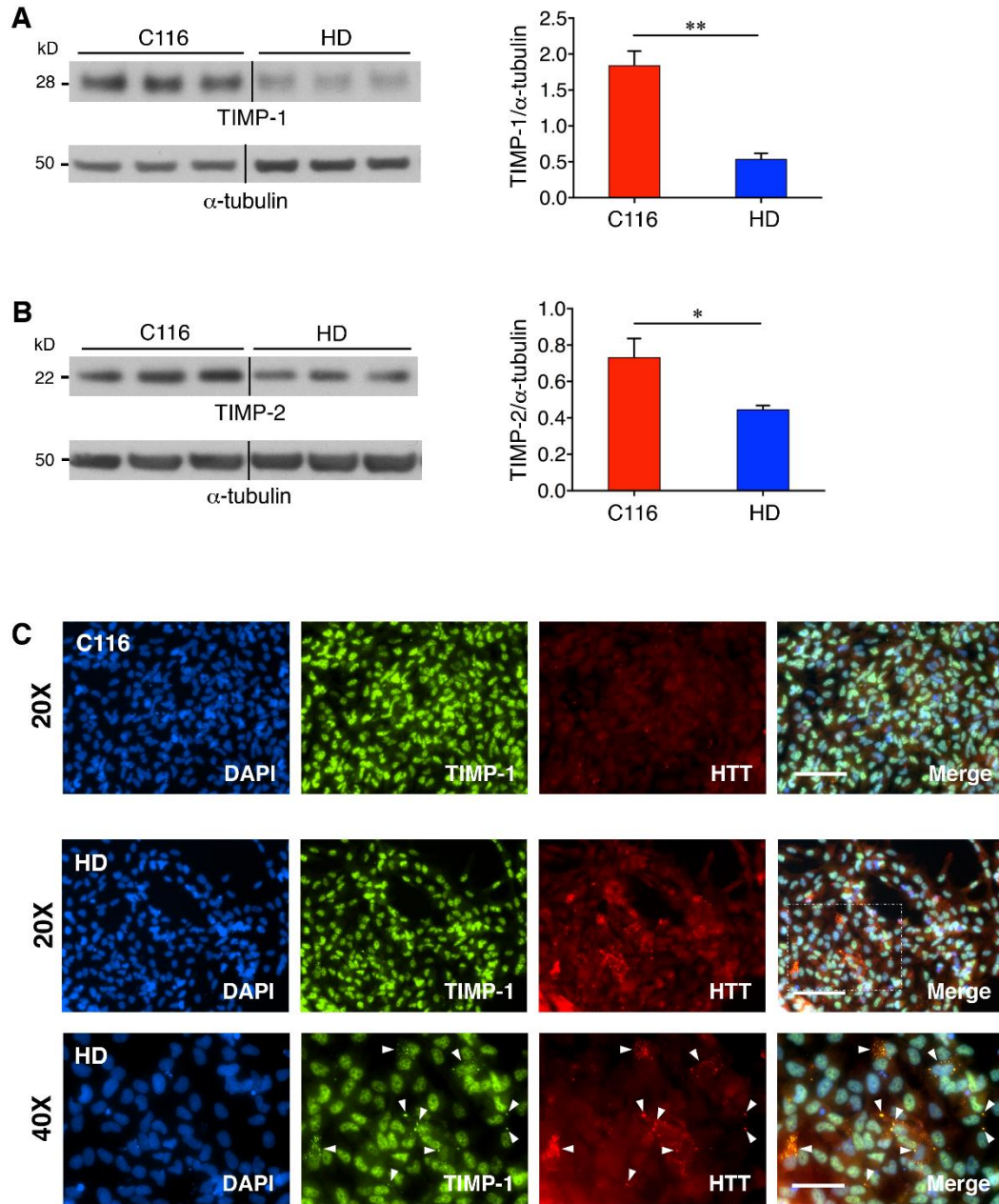


Figure 4: TIMP-1 Expression in HD-NSCs

- (A) TIMP-1 expression in HD-NSCs are lowered in HD-NSCs compared to C116-NSCs. $**p < 0.0$.
- (B) TIMP-2 expression in HD-NSCs are lowered in HD-NSCs compared to C116-NSCs. $*p < 0.05$.
- (C) Immunocytochemistry analysis shows an increase in TIMP-1 expression near degenerating nuclei. (scale bar: 20X = 100 μ m). Originally appeared in (Naphade et al., 2018).

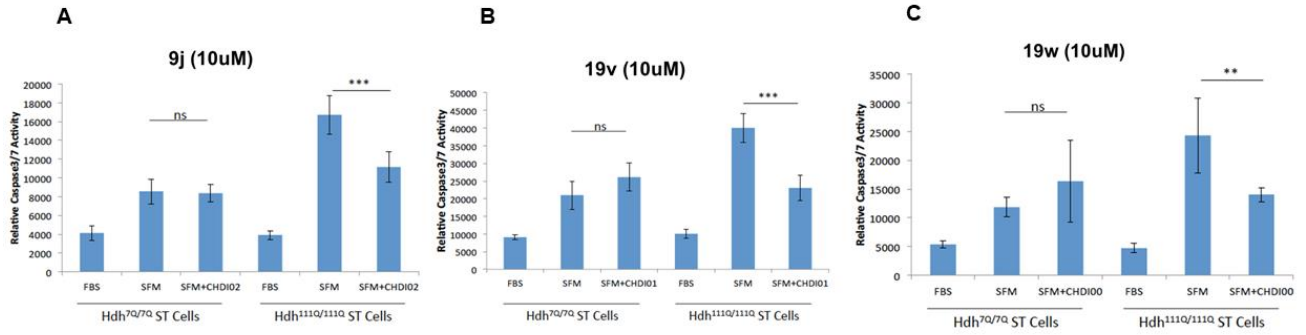


Figure 5: 9j, 19v, 19w are Neuroprotective in Mouse Striatal Cells

- (A) Quantification of caspase-3/7 relative activity measured between wild type (Hdh^{7Q/7Q}) and HD (Hdh^{111Q/111Q}) mouse striatal cells when treated with 10 μ m of MMP inhibitor compound: 9j. No significant change in normal striatal cells, *** p < 0.001 detected in CAG expanded striatal cells. Statistical analysis performed by student t-test. Error bar = SD
- (B) Quantification of caspase-3/7 relative activity measured between wild type (Hdh^{7Q/7Q}) and HD (Hdh^{111Q/111Q}) mouse striatal cells when treated with 10 μ m of MMP inhibitor compound: 19v. No significant change in normal striatal cells, *** p < 0.001 detected in CAG expanded striatal cells. Statistical analysis performed by student t-test.
- (C) Quantification of caspase-3/7 relative activity measured between wild type (Hdh^{7Q/7Q}) and HD (Hdh^{111Q/111Q}) mouse striatal cells when treated with 10 μ m of MMP inhibitor compound: 19w. No significant change in normal striatal cells, ** p < 0.01 detected in CAG expanded striatal cells. Statistical analysis performed by student t-test.

MMP Inhibitor Compounds

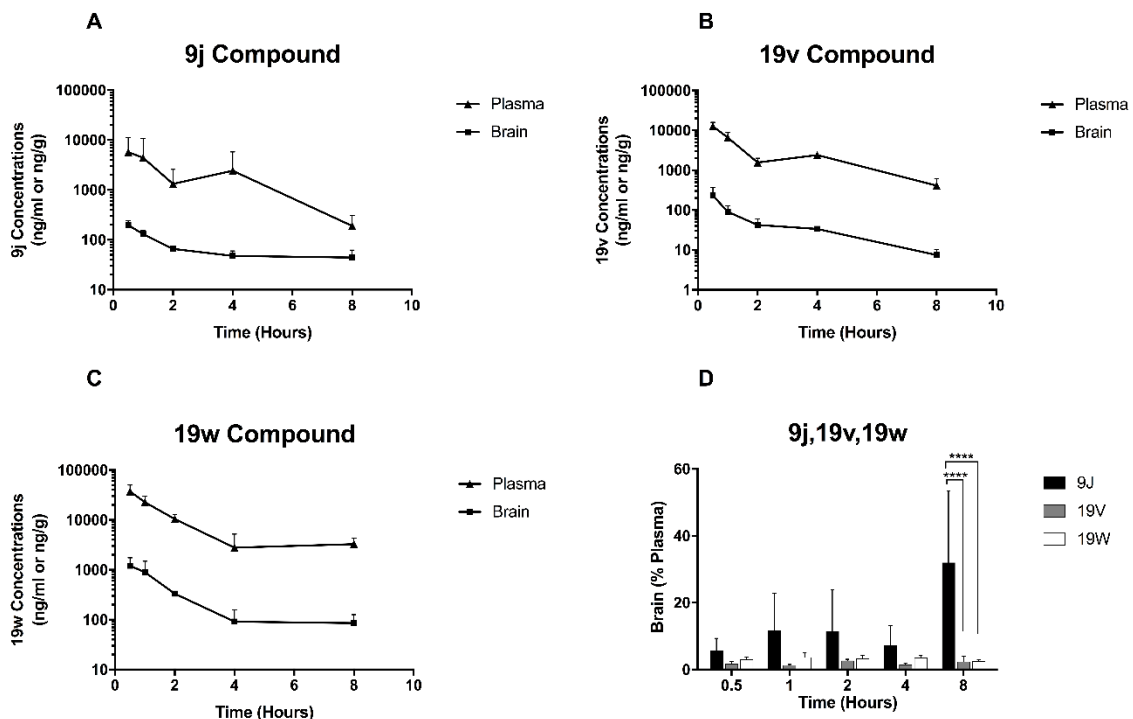


Figure 6: Pharmacokinetic Profile of MMP Inhibitor Compounds: 9j, 19v, and 19w

- (A) Plasma and brain levels of 9j compound in C57/BL6 mice after a single IP administration (25mg/kg). Levels were detected at 0.5, 1, 2, 4, and 8 hours post dosing. $n = 3$ mice/timepoint, error bars = S.D.
- (B) Plasma and brain levels of 19v compound in C57/BL6 mice after a single IP administration (25mg/kg). Levels were detected at 0.5, 1, 2, 4, and 8 hours post dosing. $n = 3$ mice/timepoint, error bars = S.D.
- (C) Plasma and brain levels of 19w compound in C57/BL6 mice after a single IP administration (25mg/kg). Levels were detected at 0.5, 1, 2, 4, and 8 hours post dosing. $n = 3$ mice/timepoint, error bars = S.D.
- (D) Inhibitor compound retained in brain tissue compared to amount in plasma levels at each timepoint (0.5, 1, 2, 4, and 8 hour post administration). $n = 3$ /timepoint. Statistical analysis performed by 2-way ANOVA, Tukey's multiple test, P value: * $p < 0.05$, **** $p < 0.0001$. Error bars = S.D.

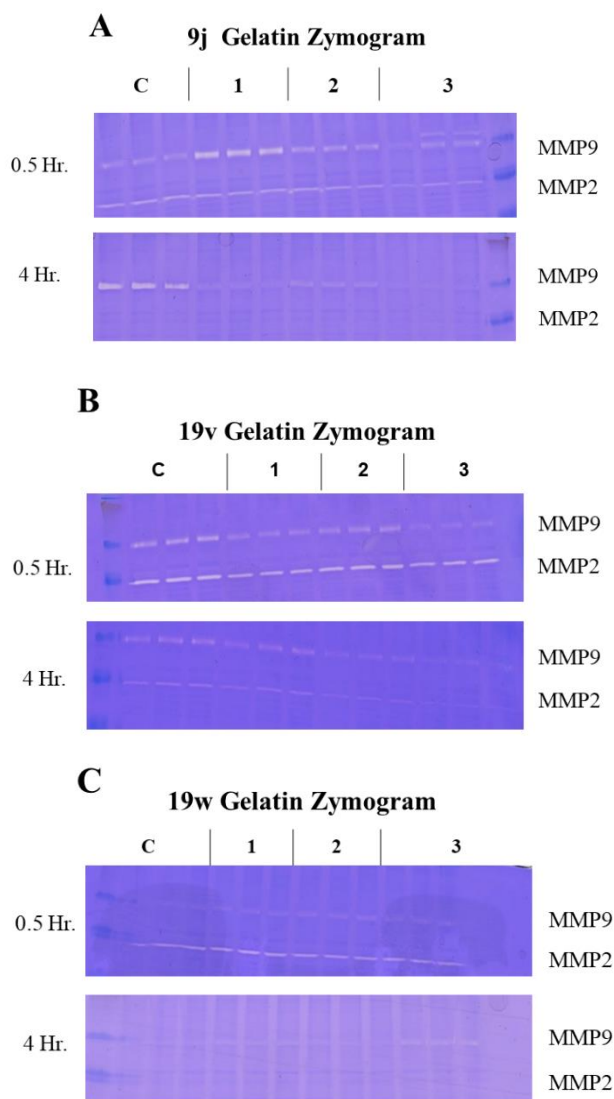


Figure 7: Visualization of MMP-2 and MMP-9 Activity by Gelatin Zymography

- (A) MMP-2 and MMP-9 activity in brain tissue at 0.5 and 4 hours post single administration of 9j compound. Visually depicts a vast decrease in MMP-2 and MMP-9 activity at later timepoint. n = 3 mice/timepoint.
- (B) MMP-2 and MMP-9 activity in brain tissue at 0.5 and 4 hours post single administration of 19v compound. Visually depicts a vast decrease in MMP-2 activity at later timepoint. n = 3 mice/timepoint.
- (C) MMP-2 and MMP-9 activity in brain tissue at 0.5 and 4 hours post single administration of 19w compound. Visually depicts a vast decrease in MMP-2 activity at later timepoint. n = 3 mice/timepoint.

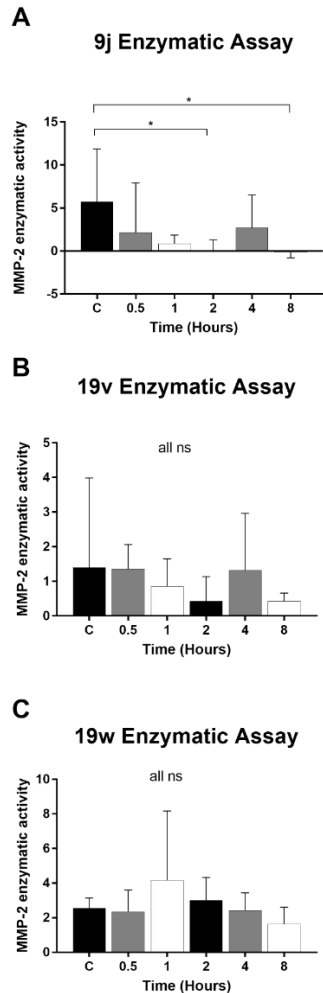


Figure 8: Measurement of MMP-2 Activity by Enzymatic Assay of Fluorogenic Substrate

- (A) Enzymatic activity of MMP-2 in brain lysates of 9j administered mice at various timepoints (0.5, 1, 2, 4, 8 hour) post single administration. Inhibition of MMP-2 was investigated by fluorescently quenched substrate (4 μ m). Enzymatic assay of 9j treated whole brain lysate was compared against 9j treated lysate with broad spectrum MMP inhibitor, 10 μ M NNGH. Overall increase in MMP-2 activity at each timepoint compared to non-9j administered control. (n = 3mice/timepoint with 3 biological replicates for each mouse). Statistical analysis by ordinary one-way ANOVA, Tukey's multiple test: * $p < 0.02$. Error bar = SD.
- (B) Enzymatic activity of MMP-2 in brain lysates of 19v administered mice at various timepoints (0.5, 1, 2, 4, 8 hour) post administration. No statistical significance.
- (C) Enzymatic activity of MMP-2 in brain lysates of 19w administered mice at various timepoints (0.5, 1, 2, 4, 8 hour) post administration. No statistical significance.

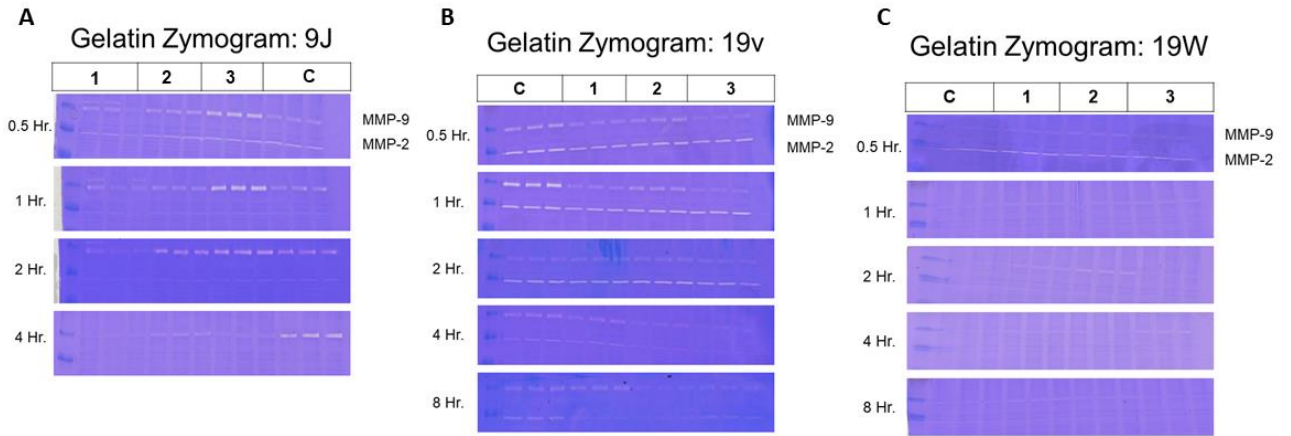


Figure 9: Gelatin Zymogram of MMP Inhibitor Administered Mice

- (A) Gelatin zymogram for 9j administered C57BL/6 mice at 0.5, 1, 2, and 4 hour timepoint representing gelatinase, MMP-2 and MMP-9, activity. n = 3 animals per timepoint, and 3 biological replicates.
- (B) Gelatin zymogram for 9v administered C57BL/6 mice at 0.5, 1, 2, 4, and 8 hour timepoint representing gelatinase, MMP-2 and MMP-9, activity. n = 3 animals per timepoint, and 3 biological replicates.
- (C) Gelatin zymogram for 19w administered C57BL/6 mice at 0.5, 1, 2, 4, and 8 hour timepoint representing gelatinase, MMP-2 and MMP-9, activity. n = 3 animals per timepoint, and 3 biological replicates.

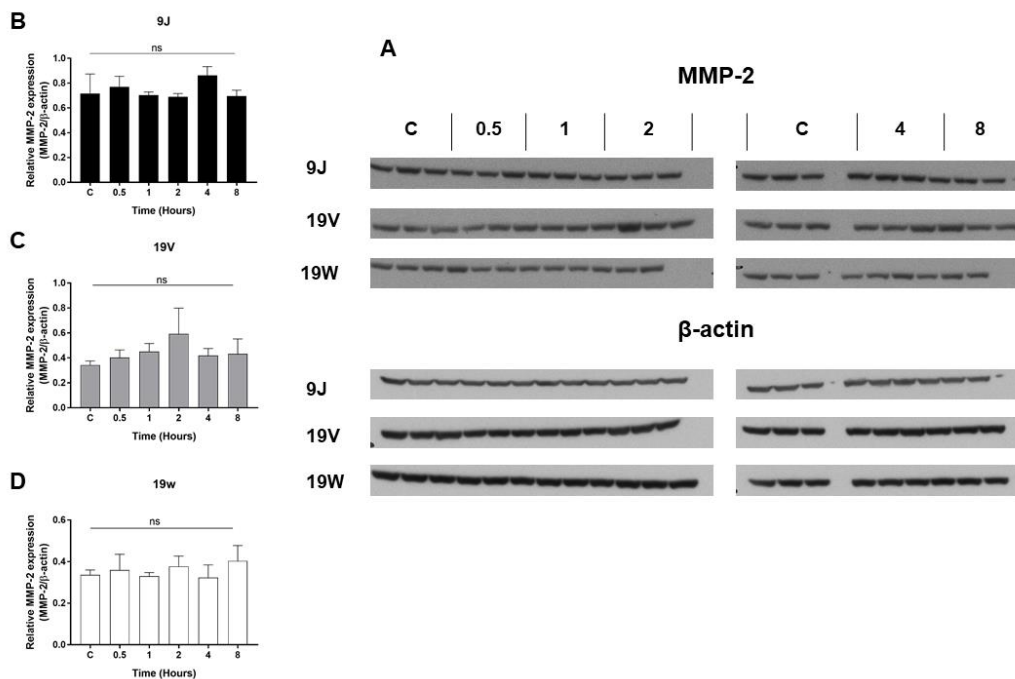


Figure 10: MMP-2 Expression of MMP Inhibitor Administered Mice

- (A) Western blot of MMP-2 expression on whole brain lysates of mice administered MMP inhibitor compound (9j, 19v, and 19w) at set timepoint (0.5, 1, 2, 4, and 8 hours) n = 3 per timepoint.
- (B) Quantification of MMP-2 expression on whole brain lysates of 9j administered mice at corresponding timepoint. Statistical analysis conducted by GraphPad prism using ANOVA, Tukey's multiple test. Error bar = SD.
- (C) Quantification of MMP-2 expression on whole brain lysates of 19v administered mice at corresponding timepoint. Statistical analysis conducted by GraphPad prism using ANOVA, Tukey's multiple test. Error bar = SD.
- (D) Quantification of MMP-2 expression on whole brain lysates of 19w administered mice at corresponding timepoint. Statistical analysis conducted by GraphPad prism using ANOVA, Tukey's multiple test. Error bar = SD.

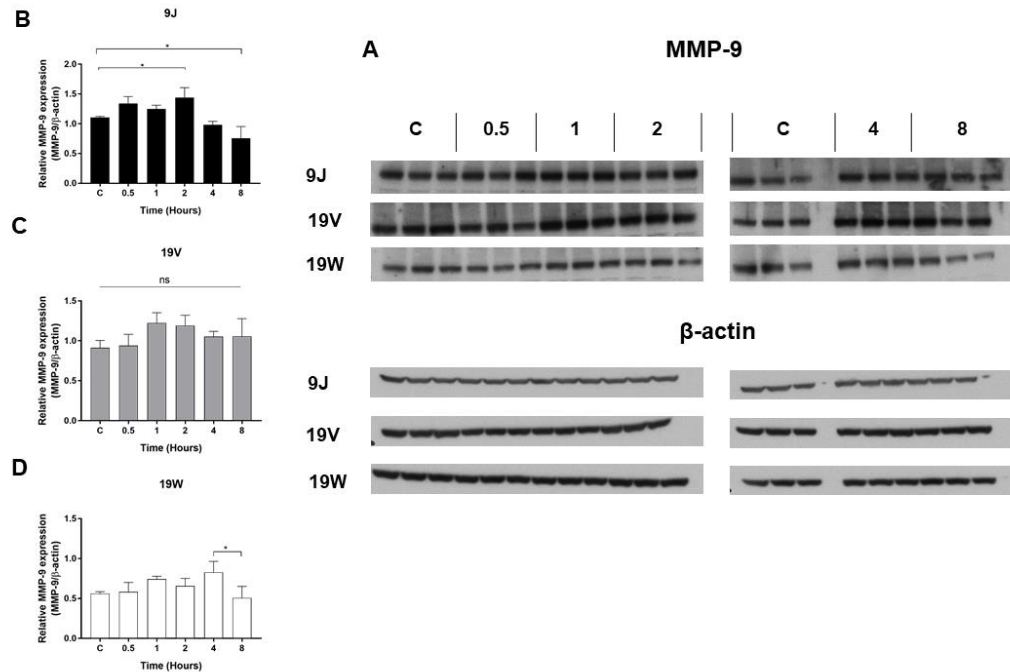


Figure 11: MMP-9 Expression in MMP Inhibitor Administered Mice

- (A) Western blot of MMP-9 expression on whole brain lysates of mice administered MMP inhibitor compound (9j, 19v, and 19w) at set timepoint (0.5, 1, 2, 4, and 8 hours) n = 3 per timepoint.
- (B) Quantification of MMP-9 expression on whole brain lysates of 9j administered mice at corresponding timepoint. Statistical analysis conducted by GraphPad prism using ANOVA, Tukey's multiple test. Error bar = SD.
- (C) Quantification of MMP-9 expression on whole brain lysates of 19v administered mice at corresponding timepoint. Statistical analysis conducted by GraphPad prism using ANOVA, Tukey's multiple test, P value: * $p < 0.05$. Error bar = SD.
- (D) Quantification of MMP-9 expression on whole brain lysates of 19w administered mice at corresponding timepoint. Statistical analysis conducted by GraphPad prism using ANOVA, Tukey's multiple test. Error bar = SD.

Chapter 2

Abstract:

Huntington's disease is an incurable genetic disorder with no current therapies. The genetic underpinning of HD is caused by a CAG expansion in exon 1 of huntingtin gene that encodes for HTT. One of the molecular pathologies of HD arises from the neurotoxicity induced by processing of mutant huntingtin into N-terminal fragments. Previous research has shown altered kinase signaling pathways to contribute to altered localization of mutant huntingtin to the nucleus and possibly disrupting the transcriptional regulation. Various protein kinase C activator compounds have been evaluated in cancers as well as Alzheimer's disease. Bryostain-1, a potent PKC activator, have done well in phase II trials and have shown to improve cognition in Alzheimer's patients. Bryostain-1 has not been evaluated in Huntington's disease and we hypothesize that PKC activation may have beneficial effects in Huntington's Disease. To determine if Bryostatin-1 has therapeutic benefit in HD, we conducted a preclinical trial in HD R6/2 mice. We measured weight, locomotion; rotarod, open field, clasping, and lifespan. R6/2 mice treated with Bryostain-1 did not show a significant improvement in locomotor ability measured by rotarod performance or measures in open field testing. However, we did find a significant increase in the average life span of Bryostain-1 HD R6/2 mice compared to vehicle treated mice. We conclude while Bryostain-1 may not benefit the deficit in locomotor ability, there is a beneficial outcome of increasing lifespan of R6/2 mice. We speculate that PKC activation may impact the regulation of seizure activity leading to an increase in lifespan. However, more experiments need to be conducted to further test this premise.

Introduction:

HD is an autosomal dominant disease that affects 1 in 10,000 people. Huntington's Disease Collaborative Research group identified the genetic cause is due to a polyglutamine expansion in the N-terminal region of the HTT protein (1993). Huntingtin gene, overall, is highly conserved from flies to mammals, however exon 1 is the least conserved region (Saudou & Humbert, 2016). The N-terminal portion of mutant huntingtin protein is susceptible to proteolytic cleavage by caspases, calpains and MMP-10, resulting in mutant N-terminal HTT cleavage fragments which have been found in post mortem brain tissue of HD patients (Mende-Mueller et al., 2001; Miller et al., 2010; Wellington et al., 2002b). Post translational modifications of huntingtin have also been shown to modulate toxicity of mHTT (Cong et al., 2011; Huang et al., 2016; Schilling et al., 2006b). For example acetylation mediates mHTT clearance and phosphorylation decreases cleavage by caspase-3 and calpains (Jeong et al., 2009; Luo, Vacher, Davies, & Rubinsztein, 2005; Saudou & Humbert, 2016). Kinase signaling has been shown to regulate the subcellular localization of huntingtin protein in mouse striatal cells (Bowles, Brooks, Dunnett, & Jones, 2015). The role of huntingtin protein in cellular processes is vast and is not fully understood. A recent review speculates that with the many interacting partners, HTT may serve as a scaffold protein by bringing multiple molecular partners to coordinate cellular processes modulated by phosphorylation events (Saudou & Humbert, 2016).

No current therapies exist to slow the progression of HD, thus one therapeutic avenue is to identify kinase inhibitors or activators as therapeutic targets for HD. Diacylglycerol

kinase ϵ (DGK ϵ) was found in a library screen of inhibitor kinases that blocked mHtt cellular toxicity in a HD mouse (Hdh^{Q111/Q111}) striatal cell line (Zhang et al., 2012).

Diacylglycerol kinases are enzymes that converts diacylglycerol (DAG) into phosphatidic acid (PA) utilizing ATP, however when DAG is not converted to PA, it is an activator of protein kinase C (PKC) (Sakane, Mizuno, Takahashi, & Sakai, 2018). Thus, the reduction of cytotoxicity in striatal cells by the inhibition of DGK ϵ might be due to the activation protein kinase C.

PKC isozymes are family of kinases that phosphorylate large number of substrates and regulate cellular processes, such as, cell proliferation, cell death, gene transcription and translation. Thus, involvement of PKC activation has been seen in various human diseases (Mochly-Rosen, Das, & Grimes, 2012). Two subgroups of PKCs, conventional and novel isoforms, are activated by DAG as well as phorbol esters, such as TPA. Impaired degradation of PKC α isoforms have been observed in cellular models of HD and is speculated to be a cause of mHtt aggregates sequestration (Zemskov & Nukina, 2003). mRNA levels of PKC β II have been shown to be reduced in R6/2 mice compared to wild type mice (Harris, Denovan-Wright, Hamilton, & Robertson, 2001). Even though there is evidence of altered levels of PKC isoforms in HD, the role of PKC activators and PKC signaling have not be fully characterized.

PKC activators have been investigated as therapeutics for many diseases by formulating compounds that target the binding of the C1 regulator domain and mimics the DG-binding, one of which is Bryostatin-1. Bryostatin-1 is a potent activator of PKC ϵ and in a Phase II clinical trial for the treatment of Alzheimer's Disease. Bryostatin-1 has been shown to increase the mini-mental state examination (Nelson et al., 2017) To test if PKC

activation is neuroprotective in HD cell models, we evaluated three known PKC activators- Prostratin, Farnesyl thiothiazole and Bryostatin-1. We found that Prostratin and Farnesyl thiothiazole were neuroprotective in our striatal HD mouse cells. Initially, we tested Prostratin in R6/2 mice and found it extended the lifespan of these mice by 20 days (data not shown). However, Prostratin has been shown to be toxic in Phase III clinical trials for AIDs. Therefore, we tested Bryostatin-1's potential as a therapeutic for HD. We evaluated Bryostatin-1 in HD R6/2 mouse model measuring rotarod, open field, weight and lifespan. We used the well characterized R6/2 HD mouse model as it has reproducible HD like phenotypes and a short lifespan (12-15 weeks) (Carter et al., 1999)

Methods:

Drug Dosage Treatment

Bryostatin-1 was administered intravenously and intraperitoneally in varying concentrations into wild type and R6/2 three-month old mice. Intravenous concentrations were delivered at 6.25 $\mu\text{g}/\text{kg}$, 12.5 $\mu\text{g}/\text{kg}$, and 15 $\mu\text{g}/\text{kg}$, intraperitoneal concentrations were 30 $\mu\text{g}/\text{kg}$, 40 $\mu\text{g}/\text{kg}$ and 50 $\mu\text{g}/\text{kg}$. Then each mouse, $n = 2$ for each concentration, was euthanized at one hour post injection and its brain harvested for western blot analysis.

Bryostatin-1 was purchased from Sigma Aldrich. R6/2 mice (Jackson Labs) were administered injections of 40 mg/kg Bryostatin-1 three times per week. Bryostatin-1 was resuspended in 10% DMSO in saline and made fresh every day. Treatment of Bryostatin-1 started at week six and continued until death. Weights of mice were measured each week. The mice were grouped as follows: $n = 15$ no-treatment, and $n = 15$ treated.

Caspase-3/7 Assay

In vitro assessment of cytotoxicity was measured in HdH^{111Q/111Q} mouse striatal cells as well as HD-NSCs of Bryostatin-1 treated cells in serum starved media. Methods for the caspase-3/7 assay are identical to that found in Chapter 1. Statistical analysis by two-tailed student t-test conducted by GraphPad prism, with 6 biological replicates.

Western Blot

Bryostatin-1 treated mice were sacrificed at one hour post injection. The brains were harvested, and the left half of the brain was homogenized in 800ul of lysis buffer (10 ml TPER, 1 tablet EDTA-free protein inhibitor, DNase1, 1.2 mM MgCl₂, 1µM expoxomycin, 100 µl phosphatase inhibitor cocktail II, 50µ MTSA, 30 nM Nicotinamide, 30 µM Sodium butyrate) and sonicated 3X for 30 seconds at 40% amplitude. Samples then were centrifuged at 14,000 rpm at 4°C and the supernatant collected for western blot analysis. Protein concentrations were measured using BCA assay (Pierce). 40 µg of total protein lysate was added to 4X LDS sample buffer (Invitrogen) and 1µl of 1M DTT and boiled for 10 minutes at 95°C. SDS-PAGE was performed on 4% – 12% NuPage Bis-Tris gel (Invitrogen). Gels were run at constant 200V for 55 minutes in MES (Invitrogen) running buffer then transferred to PVDF membrane in 1X NuPage transfer buffer and run at 20V in 4°C overnight. Membranes were then blocked in TBS with 0.1% Tween 20 (TBS-T) and 5 % non-fat milk for one hour. Primary antibody was reconstituted in 5% BSA in 1X TBS-T and then was probed overnight at 4°C, followed by incubation with secondary antibody for 3 hours at room temperature. Lastly the membranes were washed (3X) for 10 minutes and were developed using Pierce ECL (Thermo Scientific) and band

intensity was quantified by ImageQuant. Primary antibody used: Phosphorylated PKC substrate (1:1000).

Rotarod

Behavioral data collection was performed in a blind study matter. Motor performance was assessed using rotarod analysis. Initial rotarod testing was conducted prior to drug treatment and mice were randomized by their initial performance and weight into separate treatment cohorts. Rotarod assessment was conducted over three consecutive days during the light cycle at week 7, 9, 11, 13, 15, and 17. Each day consisted of a training session at constant (4 rpm) for five-minutes followed by three trial runs at accelerating speed (4 - 44 rpm) for total of 6 minutes. Statistical analysis was conducted on the third consecutive day using one-way ANOVA by GraphPad Prism software.

Open Field

Behavioral data collection was performed in a blind study matter and locomotor performance was assessed by open field. Open field assessment was conducted during the dark cycle at week 9, 12, and 15. Mice were placed in field boxes and TruScan system measured parameters in the vertical and floor plane. Recording was taken for total of ten minutes at one-minute time intervals. Analysis was conducted on the total run time of ten minutes and parameters were compared between treated and non-treated cohorts. Statistical analysis was conducted by GraphPad Prism with one-way ANOVA.

Hind Limb Clasping

Hind limb scoring was assessed in treated and non-treated groups at the end of each week. During tail suspension, normal mice will struggle as observed by flailing limb movement. Mice with neurological problems will maintain their limbs fully pressed against the body, termed clasping. Mice were lifted from the base of their tails and held straight down for ten seconds, observations were recorded, and a score was given as described below for hind limb clasping. Three readings were recorded, and the last score was taken for analysis. Scoring scale: 0 = no clasping of either hind limb for 10 second period, 1 = clasping of one hind limb, 2 = clasping of both hind limbs, 3 = both hind limbs fully clasped from initial tail suspension. Statistical analysis performed by GraphPad prism using one-way ANOVA.

Results:

We measured cytotoxicity levels of non-tumor promoting activators of PKC in serum deprived mouse HD striatal cells (Hdh^{111Q/111Q}) and HD-NSCs (**Fig. 12**). We found that Prostratin (n = 6 biological replicates) at 2 μ M ($p < 0.001$) and Farnesyl thiothiazole at 25 μ M ($p < 0.001$) significantly reduce levels of caspase-3/7 activity. However, Bryostatin-1 was not neuroprotective at the concentrations tested (**Fig. 12A**). Next, we evaluated the caspase-3/7 activity in serum deprived HD-NSCs treated with Bryostatin-1 (n = 6 biological replicates) at varying concentrations and no statistical significance was found (**Fig. 12B**). Statistical analysis was conducted by ANOVA utilizing GraphPad prism.

Initially, we conducted a preclinical trial of R6/2 mice with Prostratin based on its neuroprotective effect on the immortalized mouse HD striatal cells. We found that Prostratin resulted in an increased lifespan of the R6/2 mice suggesting it provided some

benefits to the HD mice. However, Prostratin has been reported in Phase II clinical trials in AIDS patients to have toxicity. The related drug Bryostatin-1 is in Phase III trials for AD and is safe. Therefore, we evaluated Bryostatin-1 in HD R6/2 mice. First, we performed a dose response in wild type and R6/2 mice via IP and intravenous (IV) routes of administration to determine toxicity and levels of PKC activation. We administered 30 μ g, 40 μ g, and 50 μ g intraperitoneally (n = 2 mice per concentration) and sacrificed mice after one hour post injection and collected the brains for western blot analysis to detect phosphorylated PKC substrates. We did the same dosage response via tail vein injection at 6.65 μ g, 12.5 μ g, 25 μ g, 50 μ g, and 100 μ g concentrations and visualized phosphorylated PKC substrate. Western blot analysis revealed a significant increase in phosphorylated PKC substrates at 30, 40, and 50 μ g of Bryostatin-1 administration using IP injections one-hour post injection in the brain (**Fig. 13A**). A similar increase in phosphorylated PKC substrates was detected at 50 μ g and 100 μ g of Bryostatin-1 administration using IV injection (**Fig. 13B**). Lower amounts of Bryostatin-1 administration using IV injection did not result in the phosphorylation of PKC substrates. Based on dose response with Bryostatin, we treated HD R6/2 (n =15 per group), aggressive HD mouse model, with 20 μ g of Bryostatin-1 (in 10% DMSO) using X injection three times a week starting at six weeks of age. Subsequently, we monitored and weighed the mice every week as well as assessed hind limb claspability. We also conducted locomotor assessment with rotarod every two weeks and open field testing every three weeks until death. Bryostatin-1 treated mice did on average live 20% longer than the non-treated group (**Fig. 14A**). Although the R6/2 mice lose weight as the disease progresses we did not detect a statistical difference between Bryostatin-1 and vehicle

treated mice (**Fig. 14B**). Further evaluation of the R6/2 mice treated with Bryostatin-1 and vehicle did not yield any statistical difference in rotarod (**Fig. 14C**) although there may be a slight non-statistical improvement. Evaluation of multiple parameters measured by open field assessment in R6/2 mice treated with Bryostatin-1 and vehicle (**Fig. 15**) were negative. We did not detect any change in hind limb collapse scoring with Bryostatin-1 treatment (**Fig. 14D**).

Discussion:

Bryostatin-1 has been evaluated in mice and patients as a possible therapeutic for Alzheimer's disease (AD). Treatment with Bryostatin has been shown to prevent synaptic loss and improve cognitive function (Alkon, Epstein, Kuzirian, Bennett, & Nelson, 2005; Nelson et al., 2017). Our study evaluated the effects of Bryostatin-1 of cytotoxicity in HD cell lines and behavioral effects in aggressive model of HD mice. Bryostatin-1 treatment in the HD mouse striatal cell line didn't show a significant neuroprotective effect, compared to Prostratin and Farnesyl thiothiazole, nor was the drug found to be protective in human NSCs.

There are various PKC isoforms, novel (δ , ϵ , η , and θ) and conventional (α , β II, and γ) that are regulated by various subgroups of DGK's that regulate various cellular processes in tissue specific and cell specific manner (Sakane et al., 2018). Type 1 DGK α have been reported to be involved with T-cell anergy induction, cell motility, cell growth and apoptosis, and immune response, while DGK ϵ have been reported to regulate seizure activity and long term potentials (Sakane et al., 2018; Singh et al., 2017). Thus, Bryostatin-1, a PKC activator drug, also has a selectivity towards the activation of certain PKC isoforms and have been known to have a 2-fold selectivity for PKC ϵ over PKC α ,

and δ (Mochly-Rosen et al., 2012). There have been studies that shows various ranges of effect on the CNS. For example, studies of Bryostatin-1 in Alzheimer's Phase IIA clinical trials have shown that an increase in PKC ϵ is associated with cognitive improvements evaluated by mini-mental state examination (Nelson et al., 2017). Bryostatin-1 treatment has been shown to alleviate multiple sclerosis (MS) in mouse models and *in vitro* promoted anti-inflammatory phenotypes in various immune cells (Kornberg et al., 2018). Confounding reports have also reported Bryostatin-1 to induce secretions of chemokines and proinflammatory cytokines in AID-infected astrocytes and to disrupt the BBB for the transmigration of neutrophils (Proust, Barat, Leboeuf, Drouin, & Tremblay, 2017). Nevertheless, the BBB is highly compromised in the brain of HD mice, thus we can speculate the increase in the recruitment of neutrophils via activation of PCK α to be beneficial in clearing mHTT fragments.

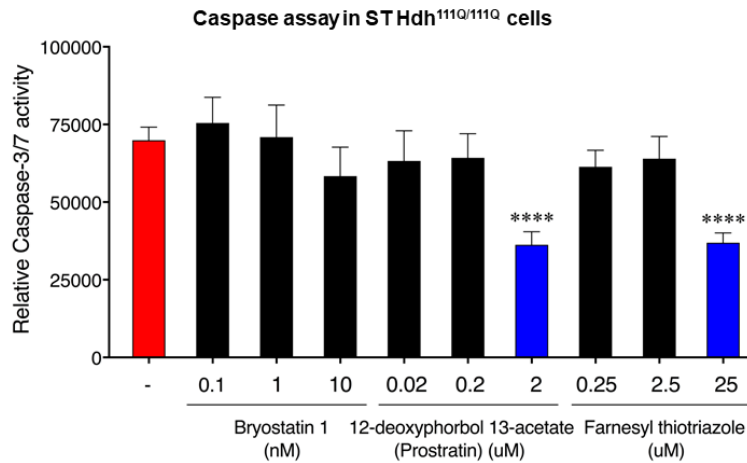
Both AD and multiple sclerosis (MS) treatment models have shown different effects of Bryostatin-1 in the targeted activation of various PCK isoforms and in different tissue and cells of the central nervous system. To this end we can speculate that the PCK isoform that is targeted by Bryostatin-1 is absent in our HD mouse striatal and human NSC models and therefore is not affected by Bryostatin-1 treatment. However, we did see activation of phosphorylated PKC substrate in our Bryostatin-1 treated wild-type and R6/2 mice suggesting a PKC family member is activated *in vivo*. While no statistical significance in the survival curve of the treated and non-treated, Bryostatin-1 treated mice did live 20% longer. This may be due to difference in seizure activity between the treated and non-treated groups during the latter stage of disease progression, as it has been shown that PKC ϵ to regulate seizure activity (Rodriguez de Turco, E B et al., 2001).

Many of the R6/2 mice have seizures that induces death and we speculate this is reduced with Bryostain-1 treatment. We did not measure this quantitatively and therefore future experiment comparing electroencephalogram (EEG) readings of Bryostatin-1 treated and non-treated might provide information of any variation in electrical signaling that takes place in the brain that may correlate to variation in seizure activity of the treated and non-treated mice. We also did not conduct studies on learning and memory in these mice and Bryostatin-1 may also impact this in R6/2 mice.

In conclusion, we detected an increase in phosphorylated PCK substrates in the brain lysates of mice administered Bryostain-1. We did not detect a neuroprotective effect of Bryostatin-1 treatment in our HD mouse striatal cells or human NSCs which may be related to dose or low levels of the target PKC family member. Our preclinical trial with Bryostatin-1 in HD R6/2 mice suggests an increase in the mean survival rate of the mice. We speculate this benefit of Bryostain-1 be through the regulation of seizure activity. We did not detect improvements in weight or motor function. Further research needs to be conducted to establish the PCK isoform, when activated, is neuroprotective and blocks seizure activity.

Tables and Figures:

A



B

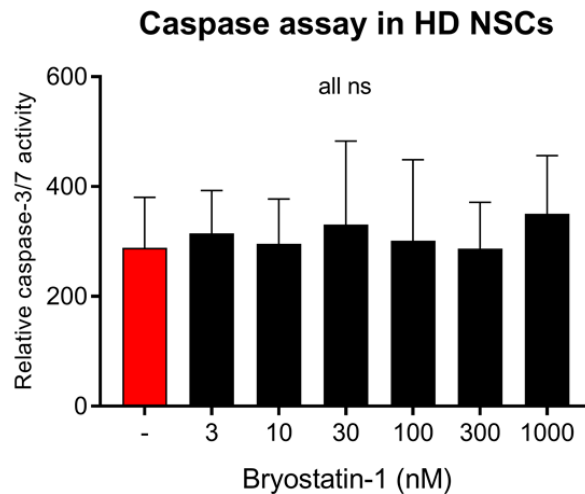


Figure 12: Cytotoxicity Evaluated in Striatal Hdh^{111Q/111Q} cells and HD-NSCs

- (A) Non-tumor promoting PKC activator, Prostratin (2 μ m) and Farnesyl thiothiazole (25 μ m) treatment in HD mouse striatal cells in serum deprived media is neuroprotective as measured by decrease in caspase-3/7 activity. student t-test, **** $p < 0.001$, $n = 6$ biological replicates (BR), error bar = SD.
- (B) Bryostatin-1 treatment in HD-NSCs in serum deprived media show no statistical significance in the reduction of caspase-3/7 activity. student t-test used for statistical analysis, $n = 6$ BR, error bar = SD.

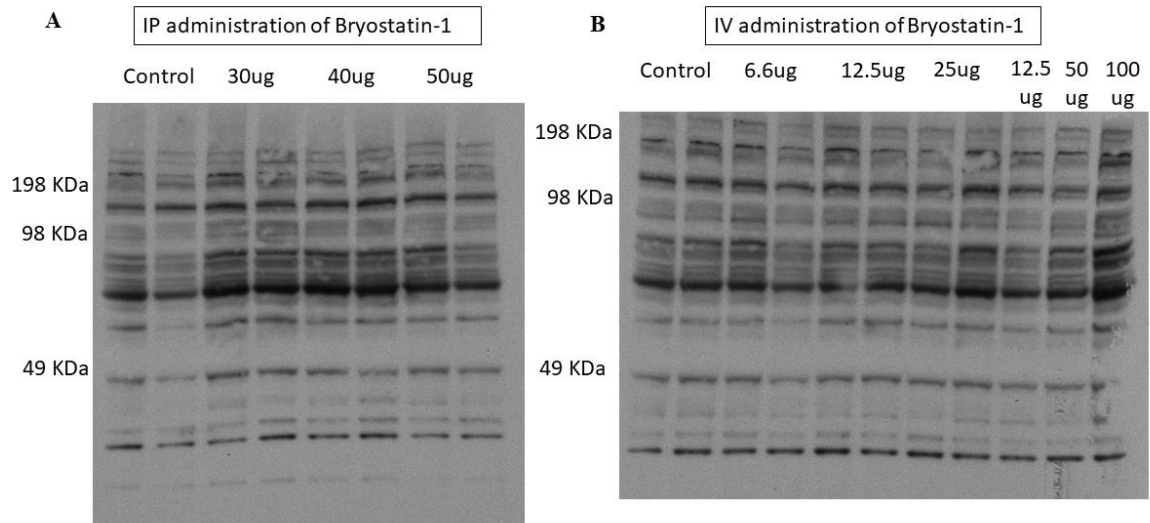


Figure 13: Bryostatin-1 Dosage Response via IP and IV Route

- (A) Bryostatin-1 administered IP at 0, 30 μg , 40 μg , and 50 μg ($n = 2$ for each dose). Western blot analysis of R6/2 brains lysates detected phosphorylated PCK substrates (49 kDa – 98 kDa) (P-(s) PKC substrate, 1:1000).
- (B) Bryostatin-1 administered IV at 0, 6.6 μg , 12.5 μg ($n = 3$), 50 μg and 100 μg ($n = 2$ for each dose). Western blot analysis of R6/2 brains lysates detected phosphorylated PCK substrates.

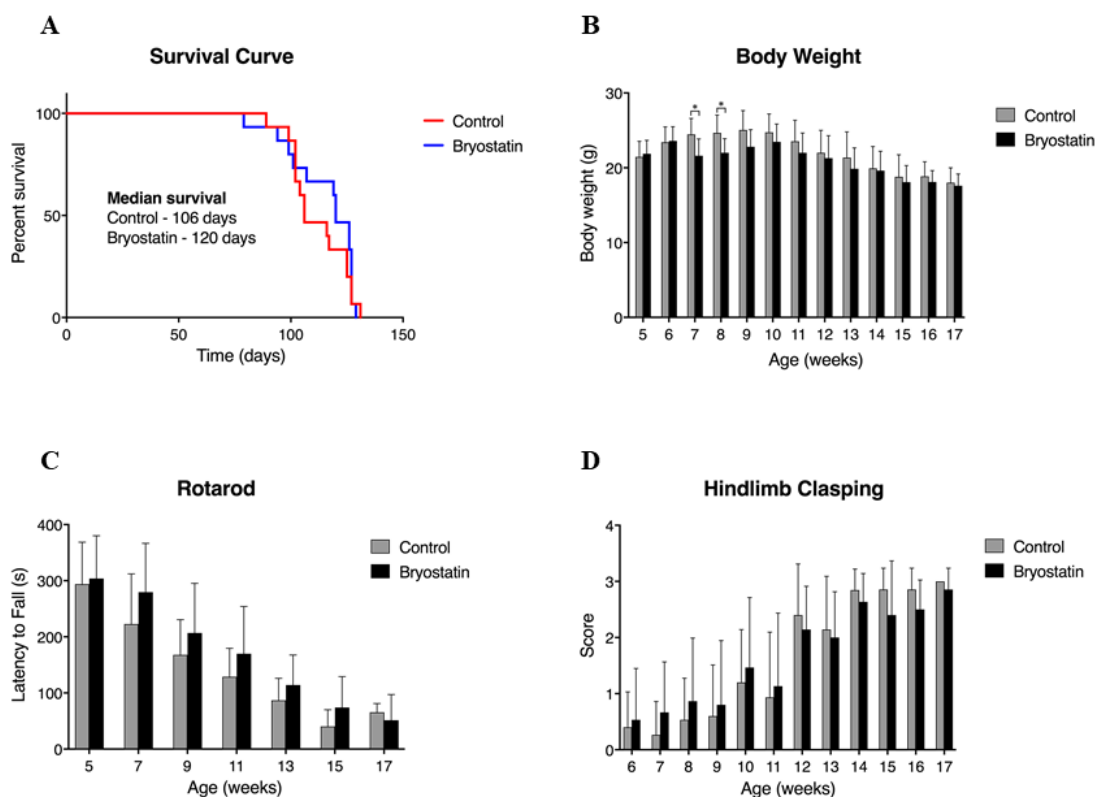


Figure 14: Behavioral Study of Bryostatin-1 Treated R6/2 Mice

- (A) Survival curve between control and Bryostatin-1 treated group ($n = 15$). Bryostatin-1 treated mice lived on average 2 weeks longer. ANOVA statistical analysis conducted by GraphPad prism. error bar =SD.
- (B) Body weight of control and Bryostatin-1 treated group. No statistical significant was measure, except at week 7 and 8, where the dosage of drug was lowered to 25 $\mu\text{g}/\text{kg}$. ANOVA statistical analysis conducted by GraphPad prism. error bar =SD.
- (C) Assessment of locomotor ability of treated and non-treated mice does not show a statistical significance in relation to an increase in age. ANOVA statistical analysis conducted by GraphPad prism. error bar =SD.
- (D) Hind limb clasping assay shows an increase in clasping of hind limbs due to age, but no statistical significance seen between the treated and non-treated. ANOVA statistical analysis conducted by GraphPad prism. error bar =SD.

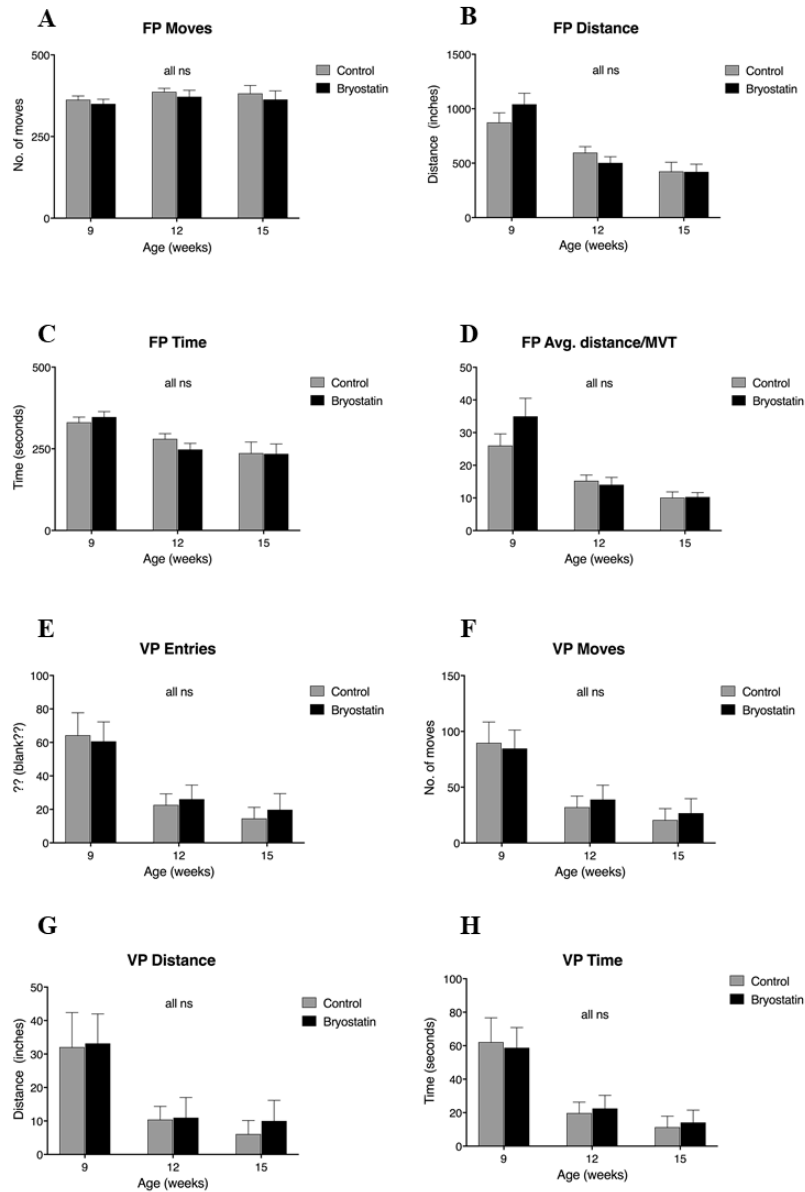


Figure 15: Open Field Testing of Bryostatin-1 Treated R6/2 mice

(A) Open field testing assessment conducted at week 9, 12, and 15 between Bryostatin-1 administered R6/2 cohorts and non-treated R6/2 mice. Parameters measured are number of moves for total of 10 minutes. (B) Distance traveled in 10 minutes, (C) Total movement time in 10 minutes, (D) Average distance per movement made, (E) number of entries made into vertical plane, (F) Total number of vertical moves made, (G) Total distance made in the vertical plane, (H) Amount of time spent in vertical plane. ANOVA statistical analysis conducted by GraphPad prism, no statistical significance. Error bar = SD

References

- Alkon, D. L., Epstein, H., Kuzirian, A., Bennett, M. C., & Nelson, T. J. (2005). Protein synthesis required for long-term memory is induced by PKC activation on days before associative learning. *Proceedings of the National Academy of Sciences of the United States of America*, *102*(45), 16432-16437. 10.1073/pnas.0508001102
- An, M. C., Zhang, N., Scott, G., Montoro, D., Wittkop, T., Mooney, S., . . . Ellerby, L. M. (2012). Genetic correction of huntington's disease phenotypes in induced pluripotent stem cells. *Cell Stem Cell*, *11*(2), 253-263. 10.1016/j.stem.2012.04.026
- Annese, V., Herrero, M., Pentima, M. D., Gomez, A., Lombardi, L., Ros, C. M., . . . Stefano, M. E. D. (2015). Metalloproteinase-9 contributes to inflammatory glia activation and nigro-striatal pathway degeneration in both mouse and monkey models of 1-methyl-4-phenyl-1,2,3,6-tetrahydropyridine (MPTP)-induced parkinsonism. *Brain Structure and Function*, *220*(2), 703-727. 10.1007/s00429-014-0718-8 Retrieved from <https://link.springer.com/article/10.1007/s00429-014-0718-8>
- Araki, Y., & Mimura, T. (2017). Matrix metalloproteinase gene activation resulting from disordred epigenetic mechanisms in rheumatoid arthritis. *International Journal of Molecular Sciences*, *18*(5), 10.3390/ijms18050905. E905 [pii]
- Becker, D. P., Barta, T. E., Bedell, L. J., Boehm, T. L., Bond, B. R., Carroll, J., . . . Yao, J. (2010). Orally active MMP-1 sparing alpha-tetrahydropyranil and alpha-piperidinyl sulfone matrix metalloproteinase (MMP) inhibitors with efficacy in

cancer, arthritis, and cardiovascular disease. *Journal of Medicinal Chemistry*, 53(18), 6653-6680. 10.1021/jm100669j [doi]

Bertini, I., Calderone, V., Fragai, M., Luchinat, C., Mangani, S., & Terni, B. (2004).

Crystal structure of the catalytic domain of human matrix metalloproteinase 10. *Journal of Molecular Biology*, 336(3), 707-716. 10.1016/j.jmb.2003.12.033

Bowles, K. R., Brooks, S. P., Dunnett, S. B., & Jones, L. (2015). Huntingtin subcellular localisation is regulated by kinase signalling activity in the StHdhQ111 model of HD. *PLoS One*, 10(12), e0144864. 10.1371/journal.pone.0144864

Brkic, M., Balusu, S., Libert, C., & Vandenbroucke, R. E. (2015). Friends or foes: Matrix metalloproteinases and their multifaceted roles in neurodegenerative diseases. *Mediators of Inflammation*, 2015, 620581. 10.1155/2015/620581 [doi]

Carter, R. J., Lione, L. A., Humby, T., Mangiarini, L., Mahal, A., Bates, G. P., . . .

Morton, A. J. (1999). Characterization of progressive motor deficits in mice transgenic for the human huntington's disease mutation. *The Journal of Neuroscience: The Official Journal of the Society for Neuroscience*, 19(8), 3248-3257.

Castellano, J. M., Mosher, K. I., Abbey, R. J., McBride, A. A., James, M. L., Berdnik, D.,

. . . Wyss-Coray, T. (2017). Human umbilical cord plasma proteins revitalize hippocampal function in aged mice. *Nature*, 544(7651), 488-492. 10.1038/nature22067

- Chang, K. H., Wu, Y. R., Chen, Y. C., & Chen, C. M. (2015). Plasma inflammatory biomarkers for huntington's disease patients and mouse model. *Brain, Behavior, and Immunity*, *44*, 121-127. 10.1016/j.bbi.2014.09.011 [doi]
- Conforti, P., Camnasio, S., Mutti, C., Valenza, M., Thompson, M., Fossale, E., . . . Cattaneo, E. (2013). Lack of huntingtin promotes neural stem cells differentiation into glial cells while neurons expressing huntingtin with expanded polyglutamine tracts undergo cell death. *Neurobiology of Disease*, *50*, 160-170. 10.1016/j.nbd.2012.10.015
- Cong, X., Held, J. M., DeGiacomo, F., Bonner, A., Chen, J. M., Schilling, B., . . . Ellerby, L. M. (2011). Mass spectrometric identification of novel lysine acetylation sites in huntingtin. *Molecular & Cellular Proteomics: MCP*, *10*(10), M111.009829. 10.1074/mcp.M111.009829
- Connolly, C., Magnusson-Lind, A., Lu, G., Wagner, P. K., Southwell, A. L., Hayden, M. R., . . . Leavitt, B. R. (2016). Enhanced immune response to MMP3 stimulation in microglia expressing mutant huntingtin. *Neuroscience*, *325*, 74-88. 10.1016/j.neuroscience.2016.03.031
- Crocker, S. J., Pagenstecher, A., & Campbell, I. L. (2004). The TIMPs tango with MMPs and more in the central nervous system. *Journal of Neuroscience Research*, *75*(1), 1-11. 10.1002/jnr.10836
- Drouin-Ouellet, J., Sawiak, S. J., Cisbani, G., Lagace, M., Kuan, W. L., Saint-Pierre, M., . . . Cicchetti, F. (2015). Cerebrovascular and blood-brain barrier impairments in

huntington's disease: Potential implications for its pathophysiology. *Annals of Neurology*, 78(2), 160-177. 10.1002/ana.24406 [doi]

Gafni, J., & Ellerby, L. M. (2002). Calpain activation in huntington's disease. *The Journal of Neuroscience: The Official Journal of the Society for Neuroscience*, 22(12), 4842-4849.

Gafni, J., Hermel, E., Young, J. E., Wellington, C. L., Hayden, M. R., & Ellerby, L. M. (2004). Inhibition of calpain cleavage of huntingtin reduces toxicity: Accumulation of calpain/caspase fragments in the nucleus. *The Journal of Biological Chemistry*, 279(19), 20211-20220. 10.1074/jbc.M401267200

Gafni, J., Papanikolaou, T., Degiacomo, F., Holcomb, J., Chen, S., Menalled, L., . . . Ellerby, L. M. (2012). Caspase-6 activity in a BACHD mouse modulates steady-state levels of mutant huntingtin protein but is not necessary for production of a 586 amino acid proteolytic fragment. *The Journal of Neuroscience: The Official Journal of the Society for Neuroscience*, 32(22), 7454-7465. 10.1523/JNEUROSCI.6379-11.2012

Hadass, O., Tomlinson, B. N., Gooyit, M., Chen, S., Purdy, J. J., Walker, J. M., . . . Gu, Z. (2013). Selective inhibition of matrix metalloproteinase-9 attenuates secondary damage resulting from severe traumatic brain injury. *PloS One*, 8(10), e76904. 10.1371/journal.pone.0076904

Harris, A. S., Denovan-Wright, E. M., Hamilton, L. C., & Robertson, H. A. (2001). Protein kinase C beta II mRNA levels decrease in the striatum and cortex of

transgenic huntington's disease mice. *Journal of Psychiatry & Neuroscience: JPN*, 26(2), 117-122.

Hermel, E., Gafni, J., Propp, S. S., Leavitt, B. R., Wellington, C. L., Young, J. E., . . .

Ellerby, L. M. (2004). Specific caspase interactions and amplification are involved in selective neuronal vulnerability in huntington's disease. *Cell Death and Differentiation*, 11(4), 424-438. 10.1038/sj.cdd.4401358

Huang, W. J., Chen, W. W., & Zhang, X. (2016). Huntington's disease: Molecular basis of pathology and status of current therapeutic approaches. *Experimental and Therapeutic Medicine*, 12(4), 1951-1956. 10.3892/etm.2016.3566 [doi]

Jeong, H., Then, F., Melia, T. J., Mazzulli, J. R., Cui, L., Savas, J. N., . . . Krainc, D.

(2009). Acetylation targets mutant huntingtin to autophagosomes for degradation. *Cell*, 137(1), 60-72. 10.1016/j.cell.2009.03.018

Kornberg, M. D., Smith, M. D., Shirazi, H. A., Calabresi, P. A., Snyder, S. H., & Kim, P.

M. (2018). Bryostatins alleviate experimental multiple sclerosis. *Proceedings of the National Academy of Sciences of the United States of America*, 115(9), 2186-2191. 10.1073/pnas.1719902115

Kwan, J. A., Schulze, C. J., Wang, W., Leon, H., Sariahmetoglu, M., Sung, M., . . .

Schulz, R. (2004). Matrix metalloproteinase-2 (MMP-2) is present in the nucleus of cardiac myocytes and is capable of cleaving poly (ADP-ribose) polymerase (PARP) in vitro. *FASEB Journal : Official Publication of the Federation of American*

Societies for Experimental Biology, 18(6), 690. 10.1096/fj.02-1202fje Retrieved from <http://www.ncbi.nlm.nih.gov/pubmed/14766804>

Leyva, M. J., Degiacomo, F., Kaltenbach, L. S., Holcomb, J., Zhang, N., Gafni, J., . . .

Ellman, J. A. (2010). Identification and evaluation of small molecule pan-caspase inhibitors in huntington's disease models. *Chemistry & Biology*, 17(11), 1189-1200. 10.1016/j.chembiol.2010.08.014

Li, Q., Michaud, M., Shankar, R., Canosa, S., Schwartz, M., & Madri, J. A. (2017).

MMP-2: A modulator of neuronal precursor activity and cognitive and motor behaviors. *Behavioural Brain Research*, 333, 74-82. S0166-4328(17)30743-X [pii]

Liao, M., & Van Nostrand, W. E. (2010). Degradation of soluble and fibrillar amyloid β -

protein by matrix metalloproteinase (MT1-MMP) in vitro. *Biochemistry*, 49(6), 1127-1136. 10.1021/bi901994d Retrieved from <https://doi.org/10.1021/bi901994d>

Loffek, S., Schilling, O., & Franzke, C. W. (2011). Series "matrix metalloproteinases in

lung health and disease": Biological role of matrix metalloproteinases: A critical balance. *The European Respiratory Journal*, 38(1), 191-208.

10.1183/09031936.00146510 [doi]

Lorenzl, S., Albers, D. S., LeWitt, P. A., Chirichigno, J. W., Hilgenberg, S. L.,

Cudkowicz, M. E., & Beal, M. F. (2003). Tissue inhibitors of matrix metalloproteinases are elevated in cerebrospinal fluid of neurodegenerative diseases. *Journal of the Neurological Sciences*, 207(1-2), 71-76.

- Luo, S., Vacher, C., Davies, J. E., & Rubinsztein, D. C. (2005). Cdk5 phosphorylation of huntingtin reduces its cleavage by caspases: Implications for mutant huntingtin toxicity. *The Journal of Cell Biology*, *169*(4), 647-656. 10.1083/jcb.200412071
- Mende-Mueller, L. M., Toneff, T., Hwang, S. R., Chesselet, M. F., & Hook, V. Y. (2001). Tissue-specific proteolysis of huntingtin (htt) in human brain: Evidence of enhanced levels of N- and C-terminal htt fragments in huntington's disease striatum. *The Journal of Neuroscience : The Official Journal of the Society for Neuroscience*, *21*(6), 1830-1837. 21/6/1830 [pii]
- Miller, J. P., Holcomb, J., Al-Ramahi, I., de Haro, M., Gafni, J., Zhang, N., . . . Ellerby, L. M. (2010). Matrix metalloproteinases are modifiers of huntingtin proteolysis and toxicity in huntington's disease. *Neuron*, *67*(2), 199-212. 10.1016/j.neuron.2010.06.021 [doi]
- Mizoguchi, H., Takuma, K., Fukuzaki, E., Ibi, D., Someya, E., Akazawa, K., . . . Yamada, K. (2009). Matrix metalloprotease-9 inhibition improves amyloid β -mediated cognitive impairment and neurotoxicity in mice. *Journal of Pharmacology and Experimental Therapeutics*, *331*(1), 14-22.
- Mochly-Rosen, D., Das, K., & Grimes, K. V. (2012). Protein kinase C, an elusive therapeutic target? *Nature Reviews. Drug Discovery*, *11*(12), 937-957. 10.1038/nrd3871
- Nagase, H., Visse, R., & Murphy, G. (2006). Structure and function of matrix metalloproteinases and TIMPs. *Cardiovascular Research*, *69*(3), 562-573.

10.1016/j.cardiores.2005.12.002 Retrieved from

<https://academic.oup.com/cardiovascres/article/69/3/562/272258>

Naphade, S., Embusch, A., Madushani, K. L., Ring, K. L., & Ellerby, L. M. (2018).

Altered expression of matrix metalloproteinases and their endogenous inhibitors in a human isogenic stem cell model of huntington's disease. *Frontiers in Neuroscience*,

1110.3389/fnins.2017.00736 Retrieved from

[https://www.frontiersin.org/articles/10.3389/fnins.2017.00736/full?utm_source=Email to authors &utm_medium=Email&utm_content=T1 11.5e1 author&utm_campaign=Email publication&field=&journalName=Frontiers in Neuroscience&id=310116](https://www.frontiersin.org/articles/10.3389/fnins.2017.00736/full?utm_source=Email%20to%20authors&utm_medium=Email&utm_content=T1_11.5e1_author&utm_campaign=Email_publication&field=&journalName=Frontiers%20in%20Neuroscience&id=310116)

Nelson, T. J., Sun, M., Lim, C., Sen, A., Khan, T., Chirila, F. V., & Alkon, D. L. (2017).

Bryostatins effects on cognitive function and PKC ϵ in alzheimer's disease phase IIa and expanded access trials. *Journal of Alzheimer's Disease: JAD*, 58(2), 521-535.

10.3233/JAD-170161

A novel gene containing a trinucleotide repeat that is expanded and unstable on

huntington's disease chromosomes. the huntington's disease collaborative research group. (1993). *Cell*, 72(6), 971-983.

O'Brien, R., DeGiacomo, F., Holcomb, J., Bonner, A., Ring, K. L., Zhang, N., . . .

Ellerby, L. M. (2015). Integration-independent transgenic huntington disease fragment mouse models reveal distinct phenotypes and life span in vivo. *The Journal of Biological Chemistry*, 290(31), 19287-19306. 10.1074/jbc.M114.623561

- Proust, A., Barat, C., Leboeuf, M., Drouin, J., & Tremblay, M. J. (2017). Contrasting effect of the latency-reversing agents bryostatin-1 and JQ1 on astrocyte-mediated neuroinflammation and brain neutrophil invasion. *Journal of Neuroinflammation*, *14*(1), 242. 10.1186/s12974-017-1019-y
- Rigamonti, D., Bauer, J. H., De-Fraja, C., Conti, L., Sipione, S., Sciorati, C., . . . Cattaneo, E. (2000). Wild-type huntingtin protects from apoptosis upstream of caspase-3. *The Journal of Neuroscience: The Official Journal of the Society for Neuroscience*, *20*(10), 3705-3713.
- Rodriguez de Turco, E B, Tang, W., Topham, M. K., Sakane, F., Marcheselli, V. L., Chen, C., . . . Bazan, N. G. (2001). Diacylglycerol kinase epsilon regulates seizure susceptibility and long-term potentiation through arachidonoyl- inositol lipid signaling. *Proceedings of the National Academy of Sciences of the United States of America*, *98*(8), 4740-4745. 10.1073/pnas.081536298
- Ross, C. A., & Tabrizi, S. J. (2011). Huntington's disease: From molecular pathogenesis to clinical treatment. *The Lancet. Neurology*, *10*(1), 83-98. 10.1016/S1474-4422(10)70245-3
- Sakane, F., Mizuno, S., Takahashi, D., & Sakai, H. (2018). Where do substrates of diacylglycerol kinases come from? diacylglycerol kinases utilize diacylglycerol species supplied from phosphatidylinositol turnover-independent pathways. *Advances in Biological Regulation*, *67*, 101-108. 10.1016/j.jbior.2017.09.003

- Saudou, F., & Humbert, S. (2016). The biology of huntingtin. *Neuron*, 89(5), 910-926.
10.1016/j.neuron.2016.02.003
- Schilling, B., Gafni, J., Torcassi, C., Cong, X., Row, R. H., LaFevre-Bernt, M. A., . . .
Ellerby, L. M. (2006a). Huntingtin phosphorylation sites mapped by mass
spectrometry. modulation of cleavage and toxicity. *The Journal of Biological
Chemistry*, 281(33), 23686-23697. 10.1074/jbc.M513507200
- Schilling, B., Gafni, J., Torcassi, C., Cong, X., Row, R. H., LaFevre-Bernt, M. A., . . .
Ellerby, L. M. (2006b). Huntingtin phosphorylation sites mapped by mass
spectrometry. modulation of cleavage and toxicity. *The Journal of Biological
Chemistry*, 281(33), 23686-23697. 10.1074/jbc.M513507200
- Singh, R. K., Kumar, S., Gautam, P. K., Tomar, M. S., Verma, P. K., Singh, S. P., . . .
Acharya, A. (2017). Protein kinase C- α and the regulation of diverse cell responses.
Biomolecular Concepts, 8(3-4), 143-153. 10.1515/bmc-2017-0005
- Stefano, M. E., & Herrero, M. T. (2016). The multifaceted role of metalloproteinases in
physiological and pathological conditions in embryonic and adult brains. *Progress in
Neurobiology*, S0301-0082(15)30100-3 [pii]
- Uchida, T., Mori, M., Uzawa, A., Masuda, H., Muto, M., Ohtani, R., & Kuwabara, S.
(2016). Increased cerebrospinal fluid metalloproteinase-2 and interleukin-6 are
associated with albumin quotient in neuromyelitis optica: Their possible role on
blood-brain barrier disruption. *Multiple Sclerosis (Houndmills, Basingstoke,
England)*, 1352458516672015 [pii]

- Vafadari, B., Salamian, A., & Kaczmarek, L. (2016). MMP-9 in translation: From molecule to brain physiology, pathology, and therapy. *Journal of Neurochemistry*, *139 Suppl 2*, 91-114. 10.1111/jnc.13415
- Vandenbroucke, R. E., & Libert, C. (2014a). Is there new hope for therapeutic matrix metalloproteinase inhibition? *Nature Reviews. Drug Discovery*, *13*(12), 904-927. 10.1038/nrd4390 [doi]
- Vandenbroucke, R. E., & Libert, C. (2014b). Is there new hope for therapeutic matrix metalloproteinase inhibition? *Nature Reviews. Drug Discovery*, *13*(12), 904-927. 10.1038/nrd4390
- Wellington, C. L., Ellerby, L. M., Gutekunst, C. A., Rogers, D., Warby, S., Graham, R. K., . . . Hayden, M. R. (2002a). Caspase cleavage of mutant huntingtin precedes neurodegeneration in huntington's disease. *The Journal of Neuroscience : The Official Journal of the Society for Neuroscience*, *22*(18), 7862-7872. 22/18/7862 [pii]
- Wellington, C. L., Ellerby, L. M., Gutekunst, C. A., Rogers, D., Warby, S., Graham, R. K., . . . Hayden, M. R. (2002b). Caspase cleavage of mutant huntingtin precedes neurodegeneration in huntington's disease. *The Journal of Neuroscience : The Official Journal of the Society for Neuroscience*, *22*(18), 7862-7872. 22/18/7862 [pii]
- Wellington, C. L., Singaraja, R., Ellerby, L., Savill, J., Roy, S., Leavitt, B., . . . Hayden, M. R. (2000). Inhibiting caspase cleavage of huntingtin reduces toxicity and

aggregate formation in neuronal and nonneuronal cells. *The Journal of Biological Chemistry*, 275(26), 19831-19838. 10.1074/jbc.M001475200

Wellington, C. L., Ellerby, L. M., Gutekunst, C., Rogers, D., Warby, S., Graham, R. K., . . . Hayden, M. R. (2002c). Caspase cleavage of mutant huntingtin precedes neurodegeneration in huntington's disease. *The Journal of Neuroscience: The Official Journal of the Society for Neuroscience*, 22(18), 7862-7872.

Zemskov, E. A., & Nukina, N. (2003). Impaired degradation of PKCalpha by proteasome in a cellular model of huntington's disease. *Neuroreport*, 14(11), 1435-1438. 10.1097/01.wnr.0000082020.91120.35

Zhang, N., Li, B., Al-Ramahi, I., Cong, X., Held, J. M., Kim, E., . . . Ellerby, L. M. (2012). Inhibition of lipid signaling enzyme diacylglycerol kinase epsilon attenuates mutant huntingtin toxicity. *The Journal of Biological Chemistry*, 287(25), 21204-21213. 10.1074/jbc.M111.321661